Research Progress and Application Prospects of MOF@MXene Composites for Electrochemical Energy Storage

Qian Zhao[1], Yuanke Li[1], Jiaxing Li[1], Wenjie Zheng[2,*]
[1]Xi'an University of Petroleum, Xi'an 710065, China
[2]School of Chemistry and Chemical Engineering, Ningxia University, Yinchuan 750021, China
*Corresponding email: 1516858143@qq.com

Abstract

The escalating global energy crisis and the accelerating integration of intermittent renewable sources have intensified the demand for advanced electrochemical energy storage (EES) systems, including high-performance supercapacitors and lithium-ion batteries (LIBs). However, the performance of contemporary EES devices is often constrained by the intrinsic limitations of conventional electrode materials, such as insufficient electrical conductivity, sluggish ion transport kinetics, and inadequate cycling stability. In this context, the strategic hybridization of metal-organic frameworks (MOFs) and two-dimensional transition metal carbides/nitrides (MXenes) has emerged as a compelling paradigm for overcoming these bottlenecks. This review provides a comprehensive and critical analysis of the recent research progress and application prospects of MOF@MXene composites in the realm of electrochemical energy storage. We commence by delineating the fundamental properties and inherent shortcomings of individual MOF and MXene components: MOFs offer exceptional specific surface areas, tunable porosity, and abundant active sites but suffer from poor intrinsic conductivity, while MXenes provide metallic conductivity and rich surface chemistry yet are prone to detrimental restacking and oxidation. The synergistic integration of these materials into MOF@MXene heterostructures effectively mitigates these individual drawbacks, yielding a unique interfacial synergy that enhances electronic conductivity, facilitates rapid ion diffusion, and reinforces structural integrity. The review systematically examines the primary synthesis methodologies for constructing MOF@MXene architectures, followed by an in-depth exploration of their charge storage mechanisms. Specifically, we analyze the cooperative interplay between electric double-layer capacitance and Faradaic pseudocapacitance in supercapacitor applications and elucidate the pathways for lithium-ion insertion/extraction, enhanced diffusion coefficients, and improved long-term cycling stability in LIB anodes. By consolidating key advancements and structure-performance correlations, this review aims to provide valuable insights and a forward-looking perspective on the rational design of next-generation MOF@MXene composites for high-energy-density, high-power, and durable electrochemical energy storage devices.

Keywords

MOF@MXene, Electrochemical energy storage, Supercapacitors, Lithium-ion batteries

Introduction

As the global energy crisis intensifies and demand for renewable energy continues to grow, electrochemical energy storage technology plays a crucial role in modern society. Not only does it provide an effective solution to energy shortages, but it also promotes the efficient utilisation of renewable energy and sustainable development. In the utilisation of intermittent energy sources such as solar and wind power, electrochemical energy storage systems can store surplus electrical energy and release it during peak demand periods, thereby achieving energy balance and a stable supply. Furthermore, electrochemical energy storage technology holds broad application prospects in fields such as electric vehicles and smart grids, providing robust technical support for the realisation of a green energy transition [1].

Current electrochemical energy storage technologies still face numerous bottlenecks. For example, the

performance of energy storage materials needs to be further improved. Existing electrode materials suffer from shortcomings in terms of electrical conductivity, ionic transport rates, and cycling stability, making it difficult for electrochemical energy storage devices to meet the growing demands of applications in terms of energy density and cycle life [2]. Cost and safety issues in energy storage systems also require urgent resolution; high material costs and complex fabrication processes limit the large-scale commercial application of electrochemical energy storage technologies. Furthermore, certain energy storage batteries pose safety risks under extreme conditions; for instance, lithium-ion batteries may undergo thermal runaway at high temperatures, potentially causing fires or explosions. These issues severely constrain the further development and application of electrochemical energy storage technologies.

Against this backdrop, MOF@MXene composites have attracted widespread attention from researchers as a novel electrochemical energy storage material. It is worth noting that (metal-organic framework) MOF materials possess a high specific surface area, tunable pore structures and abundant active sites, enabling them to provide greater contact area and active sites for electrochemical reactions, thereby enhancing the electrochemical performance of electrode materials [3]. Regrettably, however, MOF materials often exhibit poor electrical conductivity. Their internal electron conduction pathways are relatively complex and discontinuous, resulting in low electron mobility and poor overall electrical conductivity. This leads to high electrode resistance during charging and discharging, limiting the battery's charge/discharge rates and power density, and increasing energy loss [4]. In contrast, MXene materials, with their unique two-dimensional structure and excellent conductivity, can effectively improve the electronic transport properties of electrode materials. However, MXene is prone to stacking due to the strong van der Waals forces between its layers. In practical application, particularly after multiple charge-discharge cycles, the layers tend to aggregate and stack, leading to a significant reduction in the material's specific surface area. This, in turn, affects ionic transport rates and storage performance, shortening the material's service life. Furthermore, MXene exhibits poor oxidation resistance; when exposed to air, its surface readily reacts with oxygen to form an oxide layer [5]. Therefore, combining MOFs with MXene can fully exploit their synergistic effects to produce electrode materials with high conductivity, excellent ionic transport properties and good cycling stability. By compositing conductive ferrocene-based MOFs with $Ti_3C_2T_x$ MXene, researchers have successfully prepared a dual-conductive heterojunction material that exhibits high specific capacity and excellent cycling stability in lithium-ion storage [6]. MOF@MXene composites also exhibit good structural stability and tunability, allowing for structural design and performance optimisation according to different application requirements. These advantages mean that MOF@MXene composites demonstrate immense application potential in the field of electrochemical energy storage, offering new approaches and solutions for overcoming current technological bottlenecks.

This review systematically investigates MOF@MXene composites for electrochemical energy storage, combining recent advances to analyze the energy storage mechanisms of MOFs, MXenes, and their heterostructures. It first identifies the key advantages and limitations of individual materials: MOFs offer large surface area, tunable porosity, and rich active sites but suffer from low conductivity and poor stability; MXenes provide high conductivity and fast ion transport yet face severe restacking, oxidation, and limited capacity. By highlighting their complementary features, the review explains the rationality of constructing MOF@MXene composites to achieve synergistic enhancement in electrochemical performance, providing a theoretical basis for developing high-energy-density electrode materials.

On this basis, the review focuses on the applications of MOF@MXene in supercapacitors and lithium-ion batteries. For supercapacitors, it discusses how the heterostructures integrate electric double-layer capacitance and Faradaic pseudocapacitance, inhibit MXene stacking, and accelerate charge transport to improve capacitance and cycling stability. For lithium-

ion batteries, it elaborates the roles of MOF@MXene anodes in promoting Li^+ diffusion, relieving volume expansion, and enhancing cycle life. It also summarizes common modification strategies including in-situ growth, interface engineering, and structural design to optimize electrode morphology and performance.

Finally, the review outlines current challenges such as scalable green synthesis, precise interface control, and long-term stability. It further proposes future directions including high-throughput material screening, in-situ characterization, beyond-lithium battery applications, 3D electrode construction, and stability improvement. Overall, this review provides a systematic reference for the design and application of high-performance MOF@MXene energy storage materials.

MOF@MXene

An overview of MOF materials for electrochemical energy storage research

Metal-organic frameworks (MOFs) are a class of crystalline, porous solid materials comprising three-dimensional network structures formed by metal ions and multidentate organic molecules. Their electrochemical properties are highly dependent on the precise control of the material's physicochemical properties through the synthesis protocol. With a tunable pore size range of 0.5 to 2.0 nm and an exceptionally high specific surface area exceeding 3,000 m^2/g, they provide ideal pathways for ion transport. Compared to conventional materials, MOFs demonstrate broad application prospects in the field of electrochemical energy storage, particularly in lithium-ion batteries and supercapacitors. This is primarily because, when used as an anode in lithium-ion batteries, the MOF material mitigates volume expansion and enhances lithium storage performance through its porous structure. When used as the primary electrode material in supercapacitors, it utilizes its high specific surface area and active sites to improve capacitive performance. Consequently, they hold great promise for applications such as lithium-ion batteries and supercapacitors. Specifically, when used as an anode, MOFs can mitigate volume expansion through their porous framework, thereby enhancing lithium storage capacity. As electrode materials for supercapacitors, their extensive surface area helps to improve capacitive performance (Figure 1a, 1b, 1c, 1d, 1e).

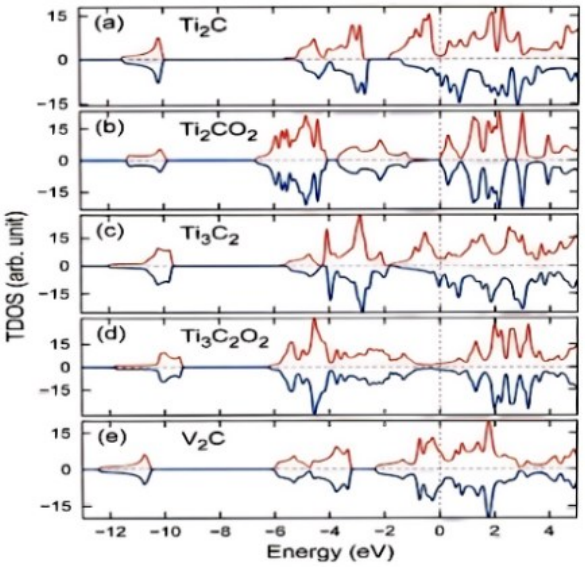

Figure 1. Density functional theory (DFT) calculated integrated electronic states as a function of energy for pristine and surface-functionalized MXenes. (a) Ti_2C, (b) Ti_2CO, (c) Ti_3C_2, (d) $Ti_3C_2O_2$, and (e) V_2C.

The data illustrates the cumulative number of electronic states up to a given energy level relative to the Fermi level (set at 0 eV). The distinct distribution observed for $Ti_3C_2O_2$ (d) reveals a significant accumulation of electronic states near the Fermi level, which is attributed to the contribution of surface - O functional groups. This enhanced density of states facilitates improved electronic conductivity and provides abundant active sites for redox reactions, thereby elucidating the origin of the superior pseudocapacitive performance observed in $Ti_3C_2T_x$ MXene electrodes compared to other transition metal carbide counterparts. In contrast, the constant unit count for V_2C (e) across the energy spectrum suggests a discrete, isolated electronic feature relevant to its specific transition metal d-orbital configuration.

The key to realizing these advantageous properties lies in the precise control of the synthesis process, as this determines the material's physicochemical properties (Figure 2a). Consequently, the design and fabrication of MOFs play a crucial role in tailoring their electrochemical behaviour (Figure 2b, 2c).

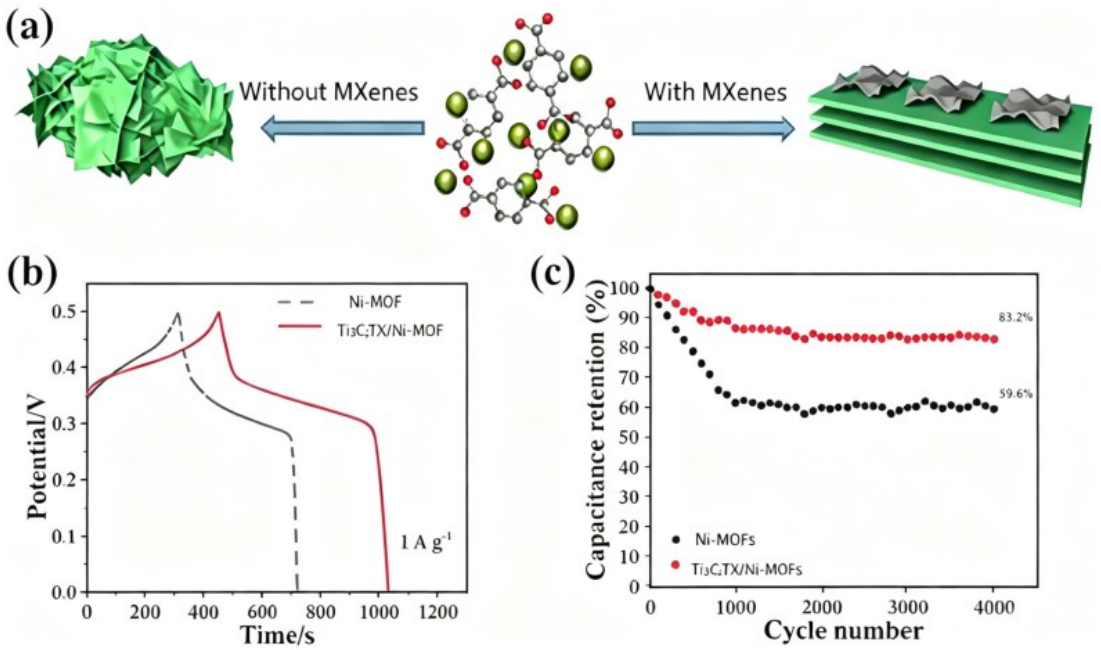

Figure 2. Effect of MXene on the structure and electrochemical performance of Ni-MOF.

(a) Schematic illustration of Ni-MOF structure without MXenes (left, aggregated structure) and with MXenes (right, layered composite structure). (b) Galvanostatic charge-discharge curves of Ni-MOF and $Ti_3C_2T_x$/Ni-MOF electrodes at a current density of 1.0 $A \cdot g^{-1}$. (c) Cycling stability comparison between Ni-MOF and $Ti_3C_2T_x$/Ni-MOF electrodes (capacitance retention vs. cycle number).

(1) Preparation of MOF materials for electrochemical energy storage research

There are various methods for synthesising MOFs, primarily including solvothermal synthesis, microwave-assisted synthesis and mechanochemical synthesis. Among these, solvothermal synthesis stands as the most widely adopted and mature approach, owing to its excellent controllability, high crystallinity, and scalability for laboratory and industrial preparation. By finely tuning the coordination environment of central metal ions, selecting appropriate solvent systems, and precisely adjusting reaction parameters such as temperature, pH, reaction time, and precursor concentration, researchers can achieve accurate regulation of the MOF's pore structure, specific surface area, crystal morphology, and surface chemical properties (Figure 3a). The electronic configuration of the metal centre, together with the type, length, and functional groups of organic ligands, collectively determines the intrinsic electrochemical properties of the resulting metal-organic framework, including conductivity, redox activity, ion affinity, and structural stability. Through rational design of the synthetic pathway and component matching, MOFs with tailored functions, such as high porosity, fast ion transport, abundant active sites, or enhanced structural robustness can be customised to satisfy the demanding requirements of diverse electrochemical energy storage applications.

Typically, using metals such as copper or zinc as the central metal, combined with organic ligands such as 2-methylimidazole or 1,3,5-benzenetricarboxylic acid, enables the directed synthesis of MOFs with specific pore sizes and functions. Lixue Yang and colleagues employed an electrochemical deposition method, using an MXene film as the working electrode, a platinum wire as the counter electrode, and Ag/AgCl as the reference electrode. In a methanol solution containing MIL-53-COOH nanocrystals and tetrabutylammonium hexafluorophosphate ((NBu4) PF6), at a current density of -8.9 $A \cdot m^{-2}$ for 300 s. This resulted in the uniform assembly of MIL-53-COOH nanocrystals on the surface of the MXene nanosheets, yielding a MIL-53-COOH/MXene hybrid film [7]. The HKUST-1 framework synthesised using Cu^{2+} and 1,3,5-benzenetricarboxylic acid, contains a large number of uncoordinated Cu^{2+} open metal sites. When HKUST-1 is combined with a polymer electrolyte, the lithium-ion transference number can be increased to over 0.6, which

is significantly superior to conventional liquid electrolyte systems; this characteristic gives it a unique advantage in the design of solid-state lithium-ion batteries (Figure 3b,3c,3d) [8].

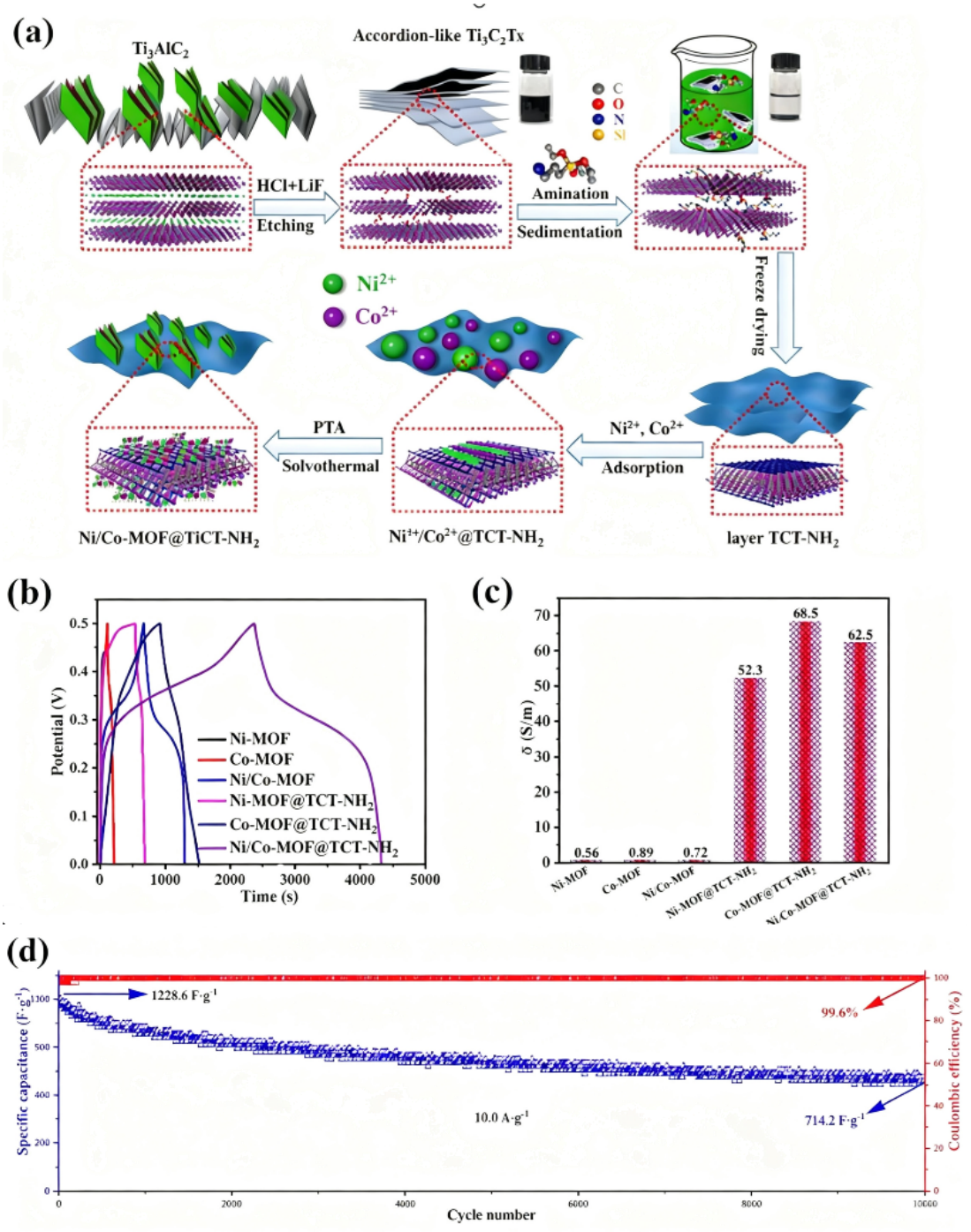

Figure 3. Synthesis procedure and electrochemical performance characterization of NiCo-MOF@TCNH$_2$ composite.

(a) Schematic illustration of the synthesis of NiCo-MOF@TCNH$_2$ from Ti_3AlC_2 via etching to accordion-like $Ti_3C_2T_x$, followed by amination, metal ion adsorption, and solvothermal reaction. (b) Galvanostatic charge-discharge curves of different electrode materials (Ni-MOF, Co-MOF, NiCo-MOF, and their composites) at a specific current density. (c) Bar chart of specific capacitance (C_s) for various electrode materials. (d) Long-term cycling stability and Coulombic efficiency of the NiCo-MOF@TCNH$_2$ electrode at a current density of 10.0 A/g.

(2) Properties of MOF materials for electrochemical energy storage research

The unique framework of MOFs, with its high specific surface area and tunable porosity, provides an ideal pathway for ion transport in electrochemical energy storage systems [9]. By selecting different metal ions such as Fe^{3+} and Co^{2+}, and adjusting the length, structure,

and functional groups of organic ligands, the pore size, pore distribution, and surface chemistry can be precisely tailored to meet the requirements of specific electrochemical applications.

In the field of electrochemistry, the open metal sites in MOFs can serve as efficient ion transport channels and provide abundant active centers for surface redox reactions. Recent advances in the design of MOF-based electrochemical materials have focused mainly on optimizing their intrinsic properties to overcome the critical limitation of low intrinsic electrical conductivity. For example, Cu^{2+}-containing MOF-74 anchors anions through unsaturated metal sites in solid-state electrolytes, significantly enhancing lithium-ion mobility and transport efficiency. Furthermore, when MOF-74 is combined with a graphene matrix, the conductivity of the composite increases sharply from 10^{-14} $S \cdot m^{-1}$ for pure MOF to 10^{-5} $S \cdot m^{-1}$, which greatly accelerates charge transfer and improves rate capability and cycling stability in electrochemical energy storage [10]. In addition, by synthesizing three types of MOFs with copper or zinc centers and ligands such as 2-methylimidazole (2MI) or 1,3,5-benzenetricarboxylic acid (H_3BTC), the two-dimensional copper-2-methylimidazole framework (2D Cu-2MI) exhibits a larger electroactive surface area, faster electron transfer capability, stronger ion adsorption capacity, and better structural stability during electrochemical cycling.

Furthermore, the rational design of MOFs with customised pore sizes and targeted functional groups can further precisely regulate ion transport kinetics and adsorption selectivity, making them highly promising candidate materials for next-generation advanced electrochemical devices. By precisely controlling the pore structure, pore size distribution, and surface chemistry of MOFs, tailored ion transport pathways and selective adsorption of specific ions can be achieved, which offers distinct advantages in high-performance battery electrolytes and supercapacitors. For example, in lithium-sulphur batteries, the hierarchical pore structure of MIL-101(Cr) restricts the shuttling effect of polysulphides via micropores with diameters smaller than 2×10^{-9} m, whilst utilising mesopores with diameters ranging from 2×10^{-9} m to 50×10^{-9} m to facilitate rapid lithium-ion diffusion, with diffusion rates reaching 1.2×10^{-12} s. This extends the battery's cycle life to over 500 cycles, with a capacity retention rate exceeding 80.0%.

Future research should continue to explore the synergistic effects of combining MOFs with other advanced functional materials, such as two-dimensional materials (graphene, MXene) and metal oxides, to further breakthrough performance limitations and enhance electrochemical stability (Figure 5a, 4a). The development of low-cost, scalable, and environmentally friendly synthesis methods, as well as in-depth investigations into long-term cycling stability under practical operating conditions, are critical steps toward the industrial application of MOF-based materials. By fully utilising the unique structural and functional advantages of MOFs, researchers can design next-generation electrochemical energy storage materials with high energy density, excellent rate capability, and long service life.

Through precise modulation of pore size and surface chemistry, MOFs enable selective ion adsorption and transport, showing significant application potential in lithium-sulphur batteries, sodium-ion batteries, and other emerging energy storage systems. For instance, the composite of MOF-5 and MXene delivers a high specific capacitance of up to 1,124 $F \cdot g^{-1}$ in supercapacitors, with over 90.0% capacitance retention after 5,000 cycles, outperforming traditional carbon-based materials that typically retain 80.0% capacity (Figure 5b, 5c).

In addition, MOF-derived carbon/Co_3O_4 composites exhibit a high open-circuit voltage of 1.52 V in zinc-air batteries, achieving a power density of 2,100 $W \cdot m^{-2}$, which represents a 30.0% performance improvement compared with commercial Pt/C catalysts (Figure 4b, 4c).

In summary, by integrating the complementary advantages of MOFs and other advanced materials, optimising scalable preparation processes, and improving long-term stability, MOF-based materials are expected to overcome the key bottlenecks of current energy storage technologies, providing innovative and reliable solutions for the development of next-generation high-performance electrochemical devices.

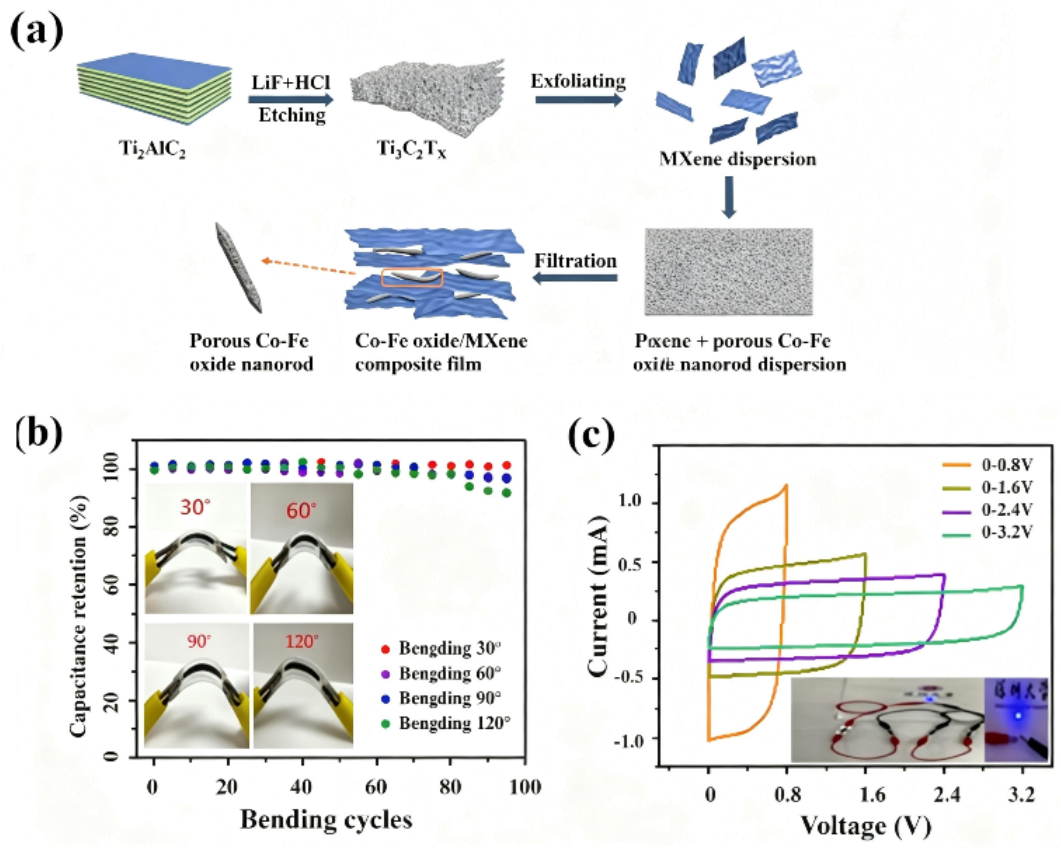

Figure 4. Fabrication and flexible electrochemical performance of porous Co-Fe oxide nanorod/MXene composite film.

(a) Schematic illustration of the fabrication process: MXene dispersion obtained by etching and exfoliating Ti_3AlC_2 is mixed with porous Co-Fe oxide nanorods, followed by vacuum filtration to prepare the composite film.

(b) Capacitance retention of the composite film after 100 bending cycles at different angles (30°, 60°, 90°, 120°) (Insets show photographs of the film under different bending angles).

(c) Cyclic voltammetry curves of the composite film at different voltage windows (0-0.8 V to 0-3.2 V) (Inset shows a photograph of the device lighting up an LED).

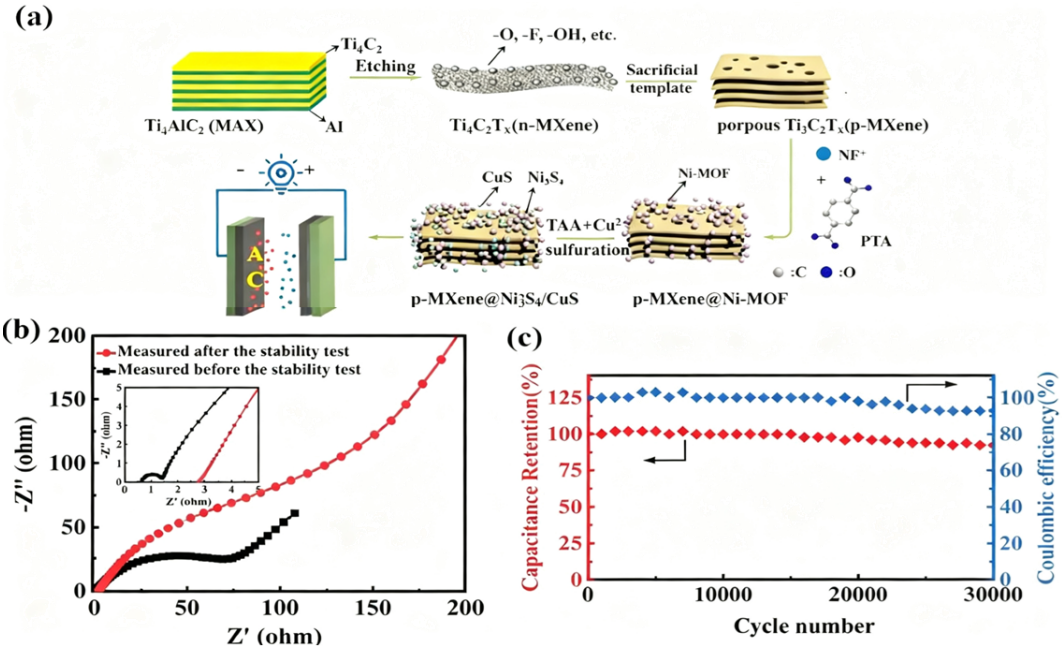

Figure 5. Synthesis procedure and electrochemical performance of p-MXene@Ni-MOF/CuS composite.

(a) Schematic illustration of the synthesis of p-MXene@Ni-MOF/CuS from Ti_3AlC_2 via preparation of porous $Ti_3C_2T_x$ (p-MXene), followed by Ni-MOF growth and sulfuration treatment (Inset shows the structure of the supercapacitor device. (b) Electrochemical impedance spectra (EIS) of the composite before and after stability test (Inset shows the magnified high-frequency region). (c) Cycling stability (capacitance retention) and Coulombic efficiency of the composite at a specific current density as a function of cycle number.

Due to their exceptionally high specific surface area, tunable pore structure and abundance of active sites, MOFs have demonstrated immense potential in the field of batteries. However, MOFs still face a number of significant challenges and shortcomings. For instance, conventional MOFs suffer from poor electrical conductivity (Figure 6a), unstable morphological characteristics during synthesis and a short service life when used in batteries (Figure 6b).

These drawbacks directly limit their direct application as battery materials.

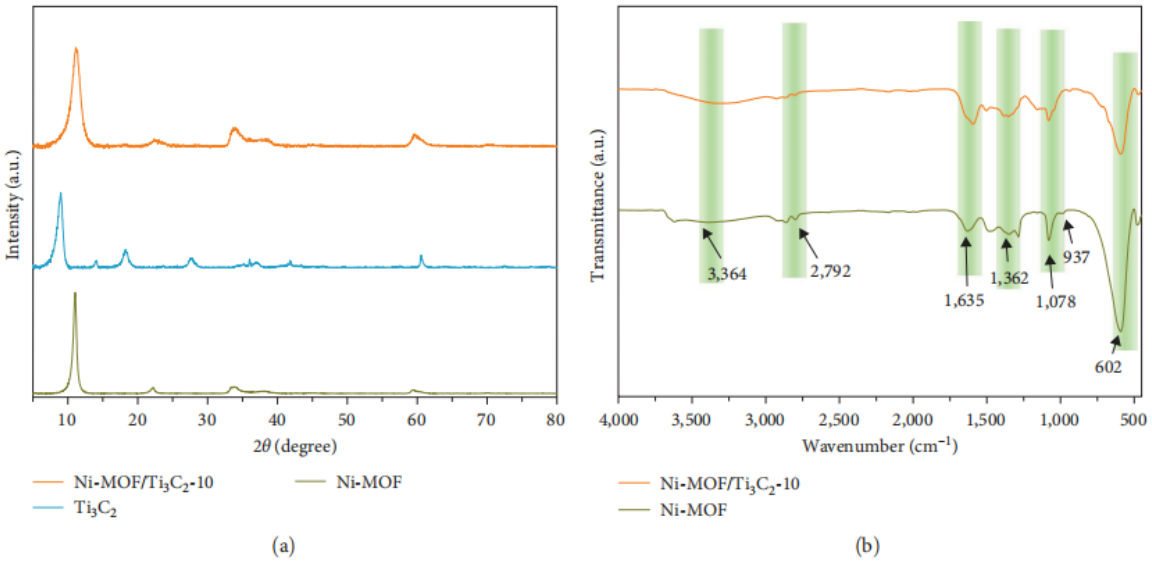

Figure 6. Structural characterization of Ni-MOF, Ti_3C_2, and Ni-MOF/ Ti_3C_2-10 composite: (a) X-ray diffraction (XRD) patterns of the three materials. (b) Fourier transform infrared (FTIR) spectra comparison between Ni-MOF and Ni-MOF/Ti_3C_2-10 composite (Characteristic vibrational peaks of functional groups are labeled).

An overview of MXene materials for electrochemical energy storage research

MXenes are a class of two-dimensional transition metal carbide/nitride materials prepared by selectively etching MAX-phase precursors. Their general chemical formula is Mn+1AX, where M represents a transition metal element, A represents a main-group element, and X represents a carbon or nitrogen atom. Due to their unique layered structure, excellent electrical conductivity and tunable surface chemistry, these materials demonstrate significant advantages in the field of supercapacitors. Taking $Ti_3C_2T_x$ MXene as an example, in a 1 $mol \cdot L^{-1}$ H_2SO_4 electrolyte system, the volumetric capacitance of this material can reach 9×10^8 $F \cdot m^{-3}$, which is significantly higher than the 2×10^8-3×10^8 $F \cdot m^{-3}$ typically observed in conventional activated carbon materials. These outstanding electrochemical properties are primarily attributable to the unique nanosheet structure and abundant surface redox active sites of MXene materials, making them an ideal choice for the development of high-power-density energy storage devices [11].

(1) Preparation of MXene materials for electrochemical energy storage research

The synthesis of MXene materials for electrochemical energy storage is primarily realized by selectively etching the A-layer from the corresponding MAX-phase precursors, typically using concentrated hydrofluoric acid (HF) or fluoride-containing salt solutions. Taking Ti_3AlC_2 as a typical example, after etching with a 40.0% HF solution at a constant temperature of 308.15 K for 24 hours, the aluminum (Al) atomic layers are selectively

and thoroughly removed, resulting in few-layer $Ti_3C_2T_x$ MXene nanosheets with a layer count below five and a lateral dimension of approximately 1 μm. Notably, MAX phases with different elemental compositions require significantly different etching conditions, mainly due to the large differences in M-A bond strength and chemical stability. For instance, between V_4AlC_3 and Ti_3AlC_2, V_4AlC_3 possesses much higher M-A bond energy and thus demands harsher etching parameters: Treatment with 50.0% HF solution at 313.15 K for 48 hours is necessary to obtain high-quality single-layer $V_4C_3T_x$. In contrast, Ti_2AlC can be efficiently exfoliated into $Ti_2C_xT_x$ nanosheets under much milder conditions - using only 30.0% HF at 303.15 K for 12 hours. These composition-dependent etching conditions are critically important for controlling layer number, structural integrity, surface terminations, and lateral size of MXene products. To obtain high-quality, few-layer or single-layer MXene nanosheets with excellent electrochemical activity, the etching parameters including acid concentration, temperature, and duration must be precisely adjusted according to the specific chemical composition and crystal structure of the parent MAX phase.

(2) Properties of MXene materials for electrochemical energy storage research

MXenes possess excellent electrical conductivity and a wealth of surface functional groups, making them suitable as carriers for a wide range of applications, including energy conversion and storage. The high metallic conductivity of MXenes stems primarily from the free electrons in the transition metal carbide or nitride framework, particularly the d-electrons of the transition metals. Furthermore, in ordered bimetallic structures, the outer-layer metals play a more significant role in electrical properties than the inner-layer metals [12]. When applying MXenes to energy storage systems, the primary considerations include scalability and electrochemical activity. MXenes are synthesised through the selective etching of MAX-phase precursors; the bond energy of the MA bonds in different MAX phases determines the etching conditions. Furthermore, as MXenes are two-dimensional (2D) materials, they have been widely used to enhance the performance of supercapacitors. Their interlayer channels and surface functional groups (such as -O and -F) can significantly enhance pseudo capacitance through redox reactions with cations (such as H^+ and Li^+). For example, compared to the 312 or 211 MAX phases (V_2AlC), the 413 MAX phase (V_4AlC_3) possesses a higher MA bond energy, thus requiring a longer etching time and a higher concentration of hydrofluoric acid (HF). In neutral and alkaline media, the volumetric capacitance is 3×10^8-4×10^8 $F\cdot m^{-3}$, outperforming pure carbon-based supercapacitors and exhibiting performance like that of activated graphene electrode materials. The shape of its cyclic voltammogram varies with the cation; in 1 $mol\cdot L^{-1}$ H_2SO_4, the volumetric capacitance of a pure layered $Ti_3C_2T_x$ clay electrode exceeds 9×10^8 $F\cdot m^{-3}$ [13].

$Ti_3C_2T_x$ MXene exhibits a volumetric capacitance of 9×10^8-1.5×10^9 $F\cdot m^{-3}$ in a 1 $mol\cdot L^{-1}$ H_2SO_4 electrolyte, far exceeding that of conventional activated carbon (2×10^8-3×10^8 $F\cdot m^{-3}$). However, the high volumetric capacitance of such materials is primarily suited to high-power applications (such as rapid charging and discharging), while their insufficient energy density (<36,000 $J\cdot kg^{-1}$) limits their application in high-energy-demand fields such as AC line filtering [14]. In electrochemical energy storage, MXenes still suffer from issues such as structural instability, limited conductivity and insufficient cycle life. However, methods such as surface chemical modification, doping, intercalation and the creation of composite materials can be used to further optimise the material structure, thereby expanding their applicability in next-generation energy storage technologies [15].

Although MXene materials have demonstrated significant potential in the field of batteries due to their high conductivity and tunable interlayer structure, their practical application still faces multiple challenges. For instance, their relatively low theoretical capacity limits the upper bound of the battery's energy density. Secondly, it is worth noting that the layers are prone to stacking, leading to a reduction in active sites and the blockage of ion transport channels, which affects rate performance and exacerbates capacity decay (Figure 7a, 7b, 7c, 7d). Insufficient chemical stability is another major challenge; MXene is prone to oxidation, particularly in aqueous

environments, and side reactions with the electrolyte reduce coulombic efficiency. In summary, there are certain difficulties in using MXene materials as a standalone battery filler (Figure 7e).

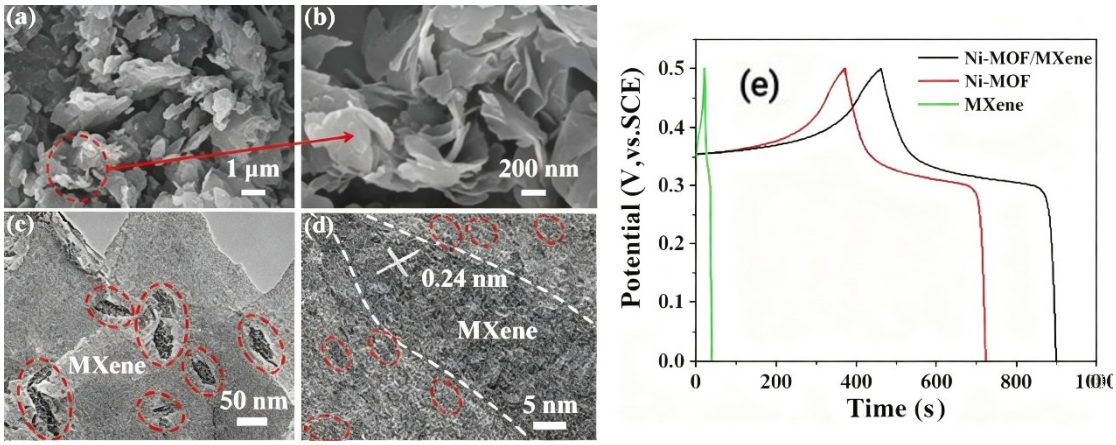

Figure 7. Microstructure and electrochemical performance characterization of Ni-MOF/ MXene composite.

(a) Scanning electron microscopy (SEM) image of the composite (low magnification). (b) Scanning electron microscopy (SEM) image of the composite (high magnification). (c) Transmission electron microscopy (TEM) image of the composite. (d) High-resolution transmission electron microscopy (HRTEM) image of the composite (showing the lattice fringes of MXene and the distribution of Ni-MOF). (e) Galvanostatic charge-discharge curves of Ni-MOF/MXene, pure Ni-MOF, and pure MXene electrodes at a specific current density.

MOF@MXene composites for electrochemical energy storage research

Although MOFs (such as ZIF-8) have emerged as promising candidates for electrochemical energy storage due to their high specific surface area (>3×10^6 $m^2\cdot kg^{-1}$), tunable pore sizes (5×10^{-10}-2×10^{-9} m) and excellent chemical stability, their intrinsic electrical conductivity is extremely low. For example, ZIF-8 has a conductivity of only ~1×10^{-8} $S\cdot m^{-1}$ - which severely limits charge transport efficiency.

Conversely, MXenes possess excellent electrical conductivity and a wealth of surface functional groups; however, they are prone to restacking due to interlayer van der Waals interactions, resulting in a loss of specific surface area and reduced utilisation of active sites. These limitations are particularly evident in energy storage devices. For example, ZIF-8-based lithium-ion electrodes exhibit sluggish ionic transport (<1×10^{-2} $S\cdot m^{-1}$), despite the presence of open Li^+ channels. Meanwhile, MXene-based supercapacitors demonstrate reduced volumetric capacitance and cycling instability due to aggregation [16].

MOF@MXene composites, however, combine the strengths of both materials, overcoming their respective shortcomings; they complement one another and demonstrate significant advantages through synergistic effects.

When MOFs and MXenes act synergistically, they offer significant advantages in energy storage. The construction of MOF/MXene composites helps prevent the restacking of MXene nanosheets. Due to the strong van der Waals forces inherent between MXene layers, two-dimensional MXene nanosheets typically exhibit an inherent tendency to restack during both synthesis and handling, driven by intense interlayer van der Waals interactions, thereby affecting the uniformity of their structure and electrochemical accessibility. This makes them highly prone to agglomeration during the preparation process or subsequent use. To address these challenges, the MOF@MXene structure synergistically integrates the advantages of both components. The porous framework of the MOF effectively mitigates MXene restacking by spatially isolating the nanosheets, thereby preserving their exposed active sites and layered porosity. Concurrently, the MXene establishes continuous conductive pathways to enhance charge transport, whilst its two-dimensional layered structure facilitates rapid ion diffusion. This complementary interaction not only eliminates the performance degradation caused by agglomeration but also optimises the accessibility of ions at the interface, collectively improving the charging and discharging efficiency and

cycling stability of lithium-ion batteries and supercapacitors.

Qu et al. proposed the use of a sonochemical method to synthesise Ni-MOF/ $Ti_3C_2T_x$ and carried out systematic morphological characterisation of the material. The authors observed that $Ti_3C_2T_x$ was uniformly distributed on the surface of the Ni-MOF, which enhanced electronic conductivity and suppressed the agglomeration of the MOF material. The study demonstrated that the Ni-MOF/ $Ti_3C_2T_x$ electrode exhibited a specific capacitance of 867.30 $F \cdot g^{-1}$ at a current density of 1.0 $A \cdot g^{-1}$. Compared with the pristine Ni-MOF material, this approach effectively improved conductivity, prevented agglomeration and enhanced electrochemical performance [17]. With regard to electrical conductivity, taking the CoN0.04-MOF-74/MXene/NF composite as an example, the material demonstrated exceptional performance in electrocatalytic activity tests for the HER (hydrogen evolution reaction) and OER (oxygen evolution reaction) in alkaline electrolytes. At current densities of 100 $A \cdot m^{-2}$ and 1,000 $A \cdot m^{-2}$, its catalytic activity significantly exceeded that of Co-MOF-74 and MXene alone, fully demonstrating the substantial advantages of the MOF@MXene composite in electrocatalysis [18].

Furthermore, during long-term energy storage, the high strength and chemical stability of the MOF@MXene composite provide structural support and protection, enhancing the overall structural stability, extending the cycle life of the energy storage device (Figure 8a, 8b, 8c, 8d), and ensuring greater reliability and durability of the composite in practical applications.

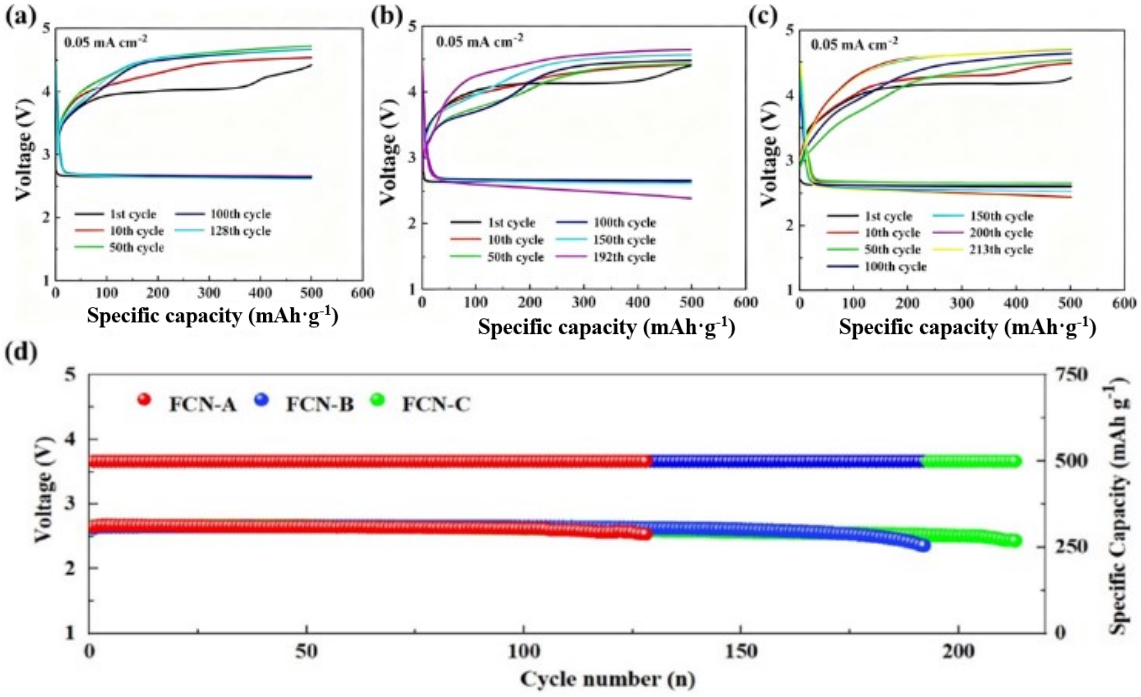

Figure 8. Electrochemical performance comparison of FCN-A, FCN-B, and FCN-C electrodes.

(a) Galvanostatic charge-discharge curves of FCN-A electrode at different cycles (1st, 50th, 100th, 128th) at a current density of 0.5 $A \cdot m^{-2}$. (b) Galvanostatic charge-discharge curves of FCN-B electrode at different cycles (1st, 50th, 100th, 192th) at a current density of 0.5 $A \cdot m^{-2}$. (c) Galvanostatic charge-discharge curves of FCN-C electrode at different cycles (1st, 50th, 100th, 150th, 200th, 213th) at a current density of 0.5 $A \cdot m^{-2}$. (d) Voltage-capacity evolution comparison of the three electrodes during cycling (showing the cycling stability and specific capacity variation of FCN-A, FCN-B, and FCN-C).

Zhang et al. designed Ni-MOF/ $Ti_3C_2T_x$ electrodes using a simple reflux method. In their study, they constructed an asymmetric supercapacitor using Ni-MOF/ $Ti_3C_2T_x$ and activated carbon as the cathode and anode, respectively. In the Ni-MOF/ $Ti_3C_2T_x$ design, MXene was employed as a structural directing agent to form a micro-ribbon morphology and prevent the agglomeration of Ni-MOF nanosheets. The final results

showed that the specific capacitances of Ni-MOF and Ni-MOF/ $Ti_3C_2T_x$ alone were 786.00 $F \cdot g^{-1}$ and 1124.00 $F \cdot g^{-1}$ respectively. This confirmed that the Ni-MOF/ $Ti_3C_2T_x$ electrode possesses excellent electrochemical performance and good cycling stability (Figure 9) [19]. Consequently, there is a need to combine MXene and MOF materials in the field of electrochemical energy storage.

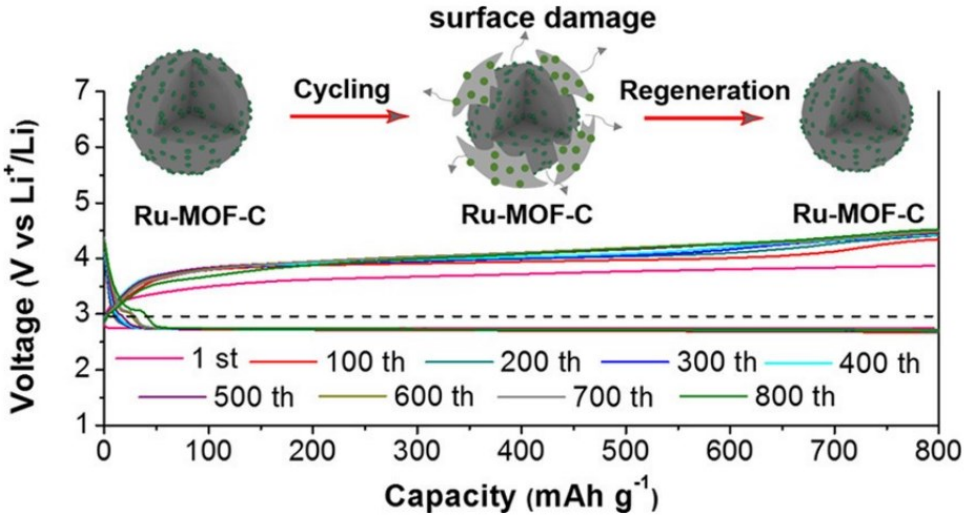

Figure 9. Structural evolution and electrochemical performance of Ru-MOF-C electrode during cycling.

The upper schematic illustrates the structural evolution of Ru-MOF-C from "surface damage" to "regeneration" during the cycling process. The lower panel shows the galvanostatic charge-discharge profiles of the Ru-MOF-C electrode at selected cycles (1st, 100th, 200th - 800th), displaying the voltage variation as a function of specific capacity (voltage range approx. 2.7-4.5 V vs Li^+/Li).

(1) Preparation of MOF@MXene composites

The strategy for preparing MOF@MXene composites aims to synergistically enhance the performance advantages of both materials through structural design and interface optimisation. The in-situ growth method is one of the mainstream approaches, involves dispersing MXene in a solvent and subjecting it to ultrasonic exfoliation, followed by the introduction of metal salts such as Co^{2+} and Ni^{2+}, along with organic ligands such as 2-methylimidazole. Under sol-gel conditions at 353.15-393.15 K, MOF crystals such as ZIF-67 are grown in an oriented manner on the MXene surface, forming a compact heterointerface that significantly enhances the material's specific surface area and electrical conductivity [20].

For applications requiring precise control of interlayer structures, the layer-by-layer self-assembly method involves chemically modifying the MXene surface and utilising electrostatic interactions or hydrogen bonding to stack MOF nanoparticles alternately with MXene layers, thereby preparing multilayer composite films. For example, HKUST-1@$Ti_3C_2T_x$ film exhibits a high areal capacitance of 2.1×104 $F \cdot m^{-2}$ in supercapacitors, whilst also demonstrating excellent cycling stability (capacitance retention >90.0% after 5,000 cycles) [21].

The electrochemical deposition method is highly suitable for the controllable and precise fabrication of electrode materials. By applying a constant voltage to a conductive substrate (such as carbon cloth) coated with MXene, the MOF precursors (such as Ni^{2+} and organic ligands) are driven to undergo uniform electrochemical nucleation on the MXene surface, forming uniform MOF nanosheets. The Ni-MOF@$Ti_3C_2T_x$ electrode prepared by this method exhibits a specific capacitance as high as 1124 $F \cdot g^{-1}$, representing a 43.0% improvement over pure MOF. Furthermore, the template method utilises the two-dimensional structure of MXene as a natural guiding template; after adsorbing metal ions, MOFs (such as MOF-5@$Ti_3C_2T_x$) are synthesised via ligand diffusion reactions, with a CO_2 adsorption capacity 30.0% higher than that of pure MOF. These methods not only resolve the interlayer stacking issue in MXene but also significantly optimise the electrochemical performance of the composite materials through strong interfacial synergy [22].

Table 1. Summary of Synthesis Methods and Electrochemical Performance of MOF/ MXene Composites.

Preparation of raw materials		Synthesis method	Performance	References
MOF raw materials	MXene raw materials			
Nickel-based metal-organic frameworks(Ni-MOF)：Ni-BDC($Ni_2(OH)_2(C_8H_4O_4)$)	$Ti_3C_2T_x$	Ultrasonic synthesis method, using high-frequency sound waves to mix Ni-MOF and $Ti_3C_2T_x$ the process takes between several tens of minutes and several hours	Ni-MOF/ $Ti_3C_2T_x$ hybrid nanosheets, specific capacitance: 867.3 F/g (1 A/g); cycling stability: 87.1% capacity retention (5,000 cycles)	[19]
MOF-5: composed of zinc ions (Zn^{2+}) and 1,4-benzenedicarboxylic acid (BDC)	V_2CT_x: prepared by etching with hydrofluoric acid (HF)	A one-step hydrothermal method: reaction of MOF-5 and V_2CT_x under high temperature and pressure, Reaction temperature: 393.15-453.15 K; reaction time: 12-24 hours.	MOF-5/ V_2CT_x Specific capacitance: 961.0 C/g (three-electrode system)	[17]
CoV_2O_6: Prepared by the thermal decomposition of ZIF-67. ZIF-67: composed of cobalt ions (Co^{2+}) and 2-methylimidazole	$Ti_3C_2T_x$	Hydrothermal and pyrolysis methods Reaction temperature: 773.15-973.15 K; reaction time: 2-4 hours	$Ti_3C_2T_x$/ ZIF-67/ CoV_2O_6 Specific capacitance: 285.5 F/g (1 A/g)	[23]
NiCo-MOF: Nickel (Ni^{2+}), Cobalt (Co^{2+})	$Ti_3C_2T_x$ - NH_2 nanosheets	Prepared by hydrothermal synthesis, Ni^{2+}- and Co^{2+}-modified $Ti_3C_2T_x$-NH_2 nanosheets were added to a solution containing 1,4-benzenedicarboxylic acid (PTA) and polyvinylpyrrolidone (PVP) and synthesised via the hydrothermal method. Reaction temperature: 393.15-453.15 K reaction time: 12-24 hours.	Ni/Co-MOF@ $Ti_3C_2T_x$ -NH_2 Specific capacitance: 2078.1 F/g (1 A/g)	[24]
Ni-MOF: composed of nickel ions (Ni^{2+})) and terephthalic acid (BDC) Ni-MOF: composed of nickel ions (Ni^{2+})) and terephthalic acid (BDC)	$Ti_3C_2T_x$	Prepared via the solvothermal method, $Ti_3C_2T_x$ and Ni-MOF react in an organic solvent; Reaction temperature: 353.15-393.15 K; reaction	$Ti_3C_2T_x$ /Ni-MOF Specific capacitance: 536 F/g (1 A/g)	[25]

Preparation of raw materials		Synthesis method	Performance	References
MOF raw materials	MXene raw materials			
		time: 12-24 hours		
Ag-MOF: composed of silver ions (Ag^{+}) and terephthalic acid (BDC)	V_2CT_x: Prepared by etching with hydrofluoric acid (HF)	Prepared via a hydrothermal method, Ag-MOF and V_2CT_x react under high temperature and pressure Reaction temperature: 393.15-453.15 K reaction time: 12-24 hours	Ag-MOF@ V_2CTx comparative capacitance：2180.0 C/g (2.0 A/g)	[23]
NiMn-MOF: composed of nickel (Ni^{2+}), manganese (Mn^{2+}) and terephthalic acid (BDC)	$Ti_3C_2T_x$	Prepared by ultrasonication; NiMn-MOF and MXene were mixed under ultrasonic conditions Between ten minutes and several hours	NiMn-MOF@MXene Capacitance：215.5 C/g (1.3 A/g)	[20]
Ni_3S_4 and CuS: prepared by the thermal decomposition of Ni-MOF	$Ti_3C_2T_x$	Prepared via a two-step process, first synthesising Ni-MOF, followed by thermal decomposition Reaction temperature: 773.15-973.15 K;reaction time: 2-4 hours	MXene@Ni_3S_4/CuS comparative capacitance：1917 F/g (1.0 A/g)	[26]

Applications of MOF@MXene in Supercapacitors

An overview of MOF@MXene materials for supercapacitor research

The rational design of MOF@MXene heterostructures has emerged as a cutting-edge strategy for developing supercapacitor electrodes with enhanced electrochemical performance by leveraging complementary charge storage mechanisms. In MOF@MXene composites, the layered porous network facilitates rapid ion diffusion. Introducing MOFs into the interlayer of MXene effectively prevents self-stacking, expands electrolyte accessibility to create more electroactive sites, and broadens the electron/ion transport pathways. Meanwhile, surface functional groups enable synergistic charge compensation, which strengthens the chemical bonding between MOFs and MXenes, thereby shortening the time required for electron/ion transport. For example, Yang et al. constructed MXene/ NiCoZDH nanosheets by immobilising nickel-exchanged ZIF-67 within MXene nanosheets. The strong chemical bonds between the MOFs and the surface functional groups of the MXene nanosheets enhanced the rates of ion diffusion and charge transfer [27].

Supercapacitors are regarded as the most promising energy storage devices; they store energy through redox reactions within the electrode materials. Given the poor electrical conductivity of metal-organic frameworks (MOFs), which severely limits the further improvement of MOF-based supercapacitor performance, this issue requires urgent attention and resolution.

In contrast, MXene materials exhibit unique advantages,

featuring a two-dimensional layered structure with distinct interlayer spacing and variable transition metal oxidation activity. These characteristics accelerate ionic reaction kinetics and allow MXenes to serve as an additional intercalation material, offering further possibilities for optimising supercapacitor performance and thereby potentially alleviating the issues caused by the insufficient conductivity of MOFs. The formation of MOF@MXene composites helps prevent the restacking and oxidation of MXene sheets, thereby enhancing the stability of the entire system. In recent years, MXene materials have been characterised by the molecular formula $Mn^{+1}XnT_x$ (where T_x denotes surface-determining groups such as O, OH, F and/or Cl bonded to the outer layer). Materials such as certain carbon nitrides and vanadium carbides possess excellent physicochemical properties; consequently, MOF@MXene heterostructures hold significant importance in supercapacitors. For example, Yang et al. proposed the synthesis of nickel-MOFs incorporating V_2CT_x (T_x).

The nickel-MOF/ V_2CT_x -modified electrode was further utilised as a supercapacitor electrode, exhibiting a specific capacitance of 1103.9 $C \cdot g^{-1}$ at 1.0 $A \cdot g^{-1}$. This electrode demonstrated acceptable cycling stability over 15,000 cycles. This stability can be attributed to the synergistic interaction between the nickel-MOF and V_2CT_x materials. In the study by Shavitaa et al., CV measurements were conducted using graphite electrodes coated with $Ti_3C_2T_x$/ Ni-MOF (10^{-30} $kg \cdot m^{-2}$) synthesised in situ.

Under low loading conditions (10 $kg \cdot m^{-2}$), the specific capacitance values were found to be high. The specific capacitance was 114.00 $F \cdot g^{-1}$. When the mass loading was 20 and 30 $kg \cdot m^{-2}$, the specific capacitances were 70.84 $F \cdot g^{-1}$ and 62.34 $F \cdot g^{-1}$, respectively, indicating an electric double-layer capacitor (EDLC) mechanism, in which charge storage is based on electrostatic interactions. The device exhibits an energy density of 19.4 $Wh \cdot g^{-1}$ and a power density of 331.8 $W \cdot g^{-1}$. Its performance is comparable to or even superior to that of other reported supercapacitor devices, and it also demonstrates excellent stability over more than 5,000 cycles [28].

The charge storage mechanism in MOF@MXene composites involves the synergistic interaction between double-layer capacitance and pseudocapacitance. Double-layer capacitance primarily relies on electrostatic interactions between the electrode material and the electrolyte, whereas pseudocapacitance arises from rapid reversible redox reactions occurring at the material's surface or within its bulk. Through their unique structural and chemical properties, MOF@MXene composites organically combine these two capacitive mechanisms, enabling highly efficient electrical energy storage and conversion. The following section will explore in detail the specific manifestations of these two capacitive mechanisms in MOF@MXene composites and the principles underlying their synergistic interaction.

Table 2. Summary of Synthesis Methods and Electrochemical Performance of MOF/ MXene Composites.

Mof@Mxene composite			Synthesis method	Capacitor performance	References
Mof raw material $Ni(NO_3)_2 \cdot 6H_2O$ $(NO_3)_2 \cdot 6H_2O$	Mxene raw material	Reaction environment			
Mof raw material $Ni(NO_3)_2 \cdot 6H_2O$ $(NO_3)_2 \cdot 6H_2O$	$fTi_3C_2T_x$	Stir vigorously at 273.15 K; in the dark	Two MOF@Ti_3C_2Tx MXene thin-film electrodes were coated with a small amount of precursor on both sides of the prepared hydrogel, which was	When ΔT=3 K: thermoelectric voltage 55.68 mV, energy conversion efficiency 3.4% When ΔT=23 K:	[29]

Mof@Mxene composite			Synthesis method	Capacitor performance	References
			then heated at 338.15 K for 15 minutes; following cooling, the TCSC was prepared.	thermoelectric voltage 131.16 mV, energy conversion efficiency 2.5%	
ZIF-67	$Ti_3C_2T_x$ nanoplates	MOF particles were grown in situ on $Ti_3C_2T_x$ nanosheets via a coprecipitation reaction, resulting in a three-dimensional $Ti_3C_2T_x$/ ZIF-67/ CO_2O_6/ AC composite material	Ti_3AlC_2 was etched at ambient temperature and pressure using a mixture of hydrochloric acid (HCl) and hydrofluoric acid (HF). The etched $Ti_3C_2T_x$ was exfoliated in deionised water. A salt solution containing Co^{2+} was mixed with a 2-methylimidazole solution, and ZIF-67 was grown in situ on the $Ti_3C_2T_x$ nanosheets via a coprecipitation reaction at ambient temperature and pressure. Under weakly alkaline conditions (e.g. pH 7-9), the Ti_3C_2Tx / ZIF-67 composite was mixed with an NH_4VO_3 solution, and the 2-methylimidazole ligands in ZIF-67 were replaced with vanadate ions via ion exchange.	Surface capacitance: 116.1-98.0 $mF·cm^{-2}$ (1^{-5} $mA·cm^{-2}$) Surface energy density: 36.27 $\mu Wh·cm^{-2}$ (0.75 $mW·cm^{-2}$) Specific capacitance: 285.50 $F·g^{-1}$ Cycle performance: 94.4% coulombic efficiency (4,000 cycles at 3.0 $A·g^{-1}$)	[30]
Ni-MOF nanosheets	Ti_3C_2Tx nanoplates	Ar gas shielding	Nickel (II) chloride hexahydrate and phthalic acid were dissolved in a DMF solution containing ethanol and deionised	Specific capacitance: 867.30 $F·g^{-1}$ ($1A·g^{-1}$) Cycle stability: 87.1%	[31]

Mof@Mxene composite			Synthesis method	Capacitor performance	References
			water. Ti_3C_2Tx and triethylamine were then added under stirring. The mixture was subsequently sonicated for 8 h under a flow of argon. Finally, the product was isolated by centrifugation and washed with ethanol, and was designated as Ni-MOF/ MXene.	capacitance retention (5,000 cycles at 5.0 $A·g^{-1}$) (Figure 10a, 10b)	
Co-MOF	Ti_3C_2Tx	Foam nickel substrate	Preparation of Ti_3C_2Tx by HF etching of Ti_3AlC_2; in situ hydrothermal synthesis (393.15 K 12 h): DMF-dispersed Ti_3C_2Tx + H_3BTC + $Co(NO_3)_2·6H_2O$	Specific capacitance: 3741.00 $F·g^{-1}$ Surface capacitance: 18.7 $F·cm^{-2}$ Cycle stability: 92.1% capacitance retention (3,000 cycles at 6 $mA·cm^{-2}$)	[32]
$NiCl_2·6H_2O$, $CoCl_2·6H_2O$, purified terephthalic acid (PTA), triethylamine (TEA)	Ti_3AlC_2 powder, which forms Ti_3C_2Tx following etching with LiF and hydrochloric acid (HCl)	Under argon (Ar) atmosphere, using DMF as the solvent, sonication at room temperature for 8 hours	Ti_3C_2Tx was mixed with Ni^{2+}/Co^{2+}, PTA and TEA, and ultrasonication was used to achieve the exfoliation of Ti_3C_2Tx and the in situ, simultaneous synthesis of the NiCo-MOF; the resulting material was then centrifuged, washed with ethanol and dried	Specific capacitance 815.2 $F·g^{-1}$ (1 $A·g^{-1}$) Energy density 39.5 $Wh·kg^{-1}$ (562.5 $W·kg^{-1}$) Power density 22.5 $kW·kg^{-1}$ (maximum) Cycle stability: 82.3% capacitance retention (5 $A·g^{-1}$, 10,000 cycles)	[33]

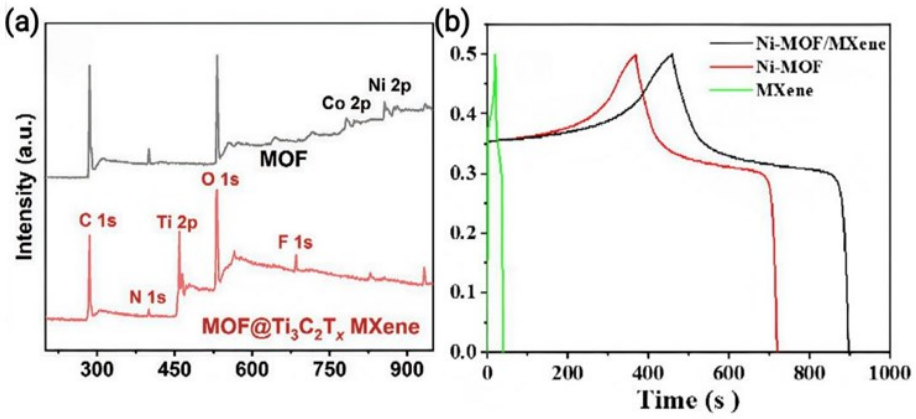

Figure 10. (a) Comparative time-dependent evolution of the normalized signal intensity for pristine Ni-MOF, pristine Ti_3C_2Tx MXene, and the Ni-MOF/ Ti_3C_2Tx hybrid nanosheets. (b) Magnified view of the intensity evolution profiles.

The Ni-MOF/ Ti_3C_2Tx composite exhibits a distinctly stable and enhanced intensity profile compared to the significant fluctuations observed in the individual Ni-MOF and MXene components. This stabilized response is indicative of the suppressed structural agglomeration and optimized interfacial synergy achieved in the hybrid architecture. The uniform distribution of MXene on the Ni-MOF surface, as confirmed by morphological characterization, facilitates continuous electronic pathways and mitigates the restacking tendencies of both constituents, thereby ensuring consistent electrochemical accessibility and long-term operational stability in energy storage applications. Reproduced with permission from Ref.

The mechanism of synergy between double-layer capacitance and Faradaic pseudocapacitance

In the field of supercapacitors, MOF@MXene composites demonstrate potential due to their exceptional performance. From an electrochemical perspective, their charge storage process involves the interaction between double-layer capacitance and Faradaic pseudocapacitance. MXene materials have attracted attention due to their two-dimensional layered structure and hydrophilic surface functional groups (Figure 11a, 11b). These characteristics enhance their ability to adsorb electrolyte ions, forming a stable double layer at the electrode surface. The introduction of MOFs not only widens the interlayer spacing of MXene but also provides a microporous structure, facilitating ion diffusion and transport, and creating conditions for the formation of double-layer capacitance (Figure 11c, 11d). Concurrently, the MOF@MXene composite integrates double-layer capacitance and pseudocapacitance through its chemical properties. Pseudo-Faradaic capacitance arises from reversible redox reactions at the material's surface or within its bulk, and the high conductivity of MXene combined with the porosity of MOFs can enhance this pseudo-capacitive effect. This synergistic effect enables the MOF@MXene composite to achieve efficient electrical energy storage and conversion in supercapacitors, offering directions for enhancing the supercapacitor performance.

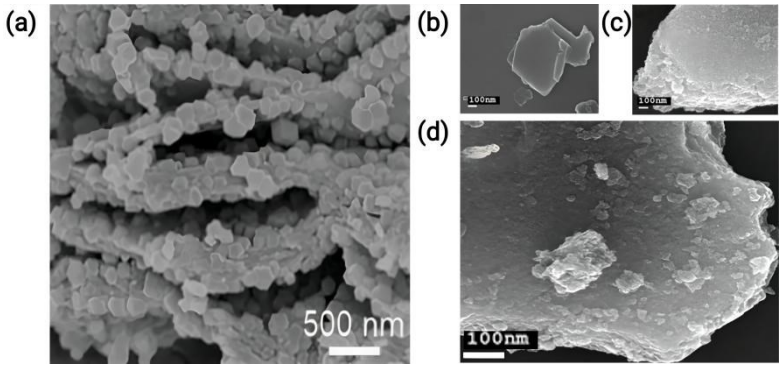

Figure 11. Morphological characterization of the Ni-MOF/ Ti_3C_2Tx nanosheets synthesized via a sonochemical method. (a, b) Scanning electron microscopy (SEM) images at different magnifications reveal the uniform distribution

and intimate interfacial contact between the Ni-MOF matrix and the exfoliated $Ti_3C_2T_x$ MXene nanosheets. Scale bars: (a) 500 nm, (b) 100 nm. (c, d) Transmission electron microscopy (TEM) images further confirming the successful integration of Ti_3C_2Tx within the Ni-MOF framework.

The MXene nanosheets serve as a conductive backbone, effectively preventing the self-agglomeration of the Ni-MOF particles while the porous MOF structure mitigates the restacking tendency of the 2D MXene layers. This well-defined heterostructure ensures the formation of continuous electronic pathways and abundant electrolyte-accessible interfaces, thereby contributing to the enhanced specific capacitance and cycling stability observed in supercapacitor applications. Reproduced with permission from Ref.

There is a fundamental difference in the operating principles of Faradaic and non-Faradaic charge storage mechanisms. The former involves redox reactions (either within the material or on its surface) that adhere to Faraday's laws, whilst the latter is a physical mechanism that does not involve redox reactions, known as double-layer capacitance (EDL) (Figure 12a).

The double-layer capacitance mechanism relies on charge separation within the polarised double layer; the double-layer capacitance (F/g) can be estimated based on the accessible surface area.

$$C_{dl} = C_A \cdot A \quad (1)$$

C_A refers to surface capacitance (typically between 50,000 and 200,000 $mF \cdot m^{-2}$, depending on the solvent and material); A is the specific surface area (SSA) (m^2/g) obtained from gas adsorption analysis (Figure 12b) [34].

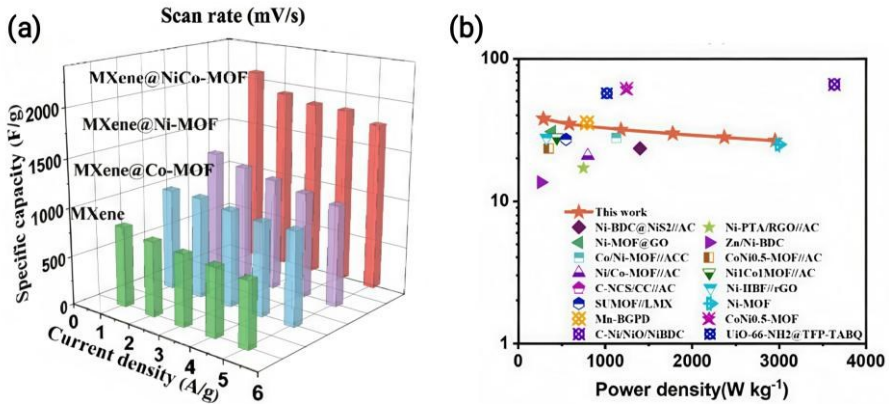

Figure 12. Ragone plot comparing the energy and power densities of the Ni-MOF/ $Ti_3C_2T_x$ hybrid electrode (denoted as "This work") with previously reported MOF-based and MXene-based supercapacitor electrodes. The data illustrate the specific energy density ($Wh \cdot kg^{-1}$) as a function of power density ($W \cdot kg^{-1}$). The Ni-MOF/$Ti_3C_2T_x$ composite demonstrates a superior energy density across a wide power range, outperforming comparative systems such as Ni-BDC@NiS_2/AC, Ni-MOF@GO, and Co/Ni-MOF/ACC. This enhanced performance is attributed to the synergistic integration of the high surface area Ni-MOF and the conductive $Ti_3C_2T_x$ MXene network, which facilitates rapid ion diffusion and efficient charge transfer while mitigating the restacking issues inherent to pristine MXenes. The plot underscores the potential of the MOF@MXene heterostructure for achieving both high energy and high power delivery in advanced electrochemical energy storage devices. Data for comparison materials were adapted from corresponding literature reports. Reproduced with permission from Ref.

SSA refers to the actual surface area occupied by a material per unit mass or volume. Liu et al. developed a general method that is highly effective for successfully synthesising uniform three-dimensional MXene/ MOF composites. These three-dimensional MOFs are crucial for preventing the aggregation and self-assembly of MXene nanosheets, thereby enhancing the transport and diffusion of MXene and electrolyte ions (Figure 13a, 13b). This structure demonstrates the great potential to enhance electrochemical performance through the synergy of customised active sites and improved structural design. (Figure 13c, 13d, 13e, 13f) The ZIF-8@MXene composite electrode exhibits significant pseudocapacitive behaviour attributable to Faradaic redox processes [33].

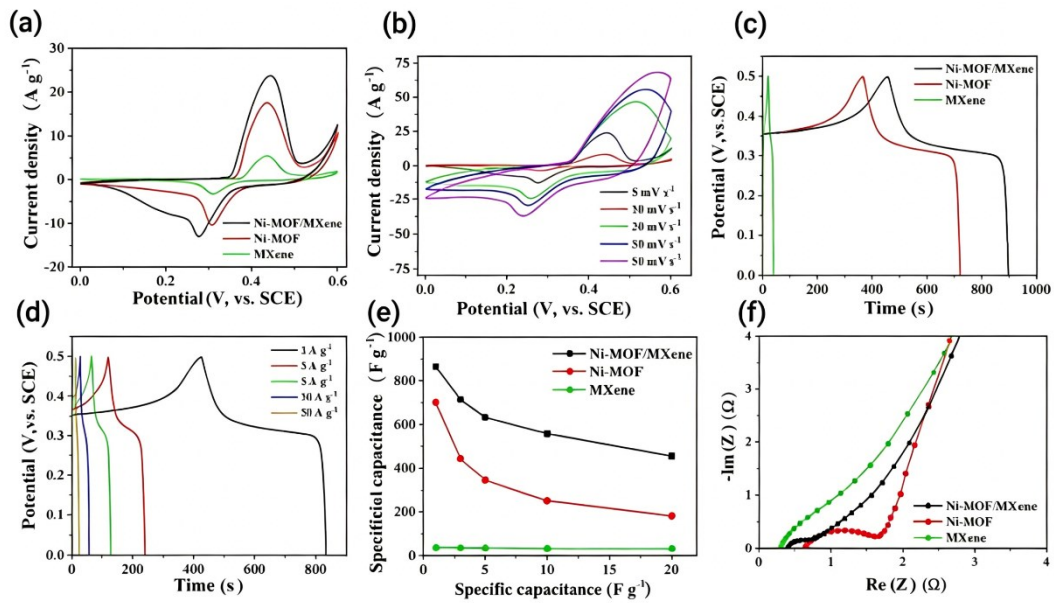

Figure 13. Summary of the anodic and cathodic peak positions and corresponding peak current densities extracted from cyclic voltammetry (CV) curves of the Ni-MOF/ $Ti_3C_2T_x$ hybrid electrode recorded at various scan rates.

The shift in peak potential and the proportional increase in peak current with scan rate reflect the rapid Faradaic redox kinetics facilitated by the MOF@MXene heterostructure. Analysis of the power-law relationship between peak current (i) and scan rate (v) ($i = av^b$) derived from data can be used to decouple the contributions from surface-controlled capacitive processes and diffusion-limited intercalation, thereby elucidating the dominant charge storage mechanism. The well-defined and stable peak currents observed across the range of scan rates indicate that the integration of the conductive $Ti_3C_2T_x$ MXene network with the electroactive Ni-MOF significantly enhances electron transport efficiency and mitigates the internal resistance typically associated with pristine MOF electrodes.

Synergistic interactions within the Ni/Co-MOF facilitate rapid redox reactions for Faradaic capacitance. The Ni/Co-MOF@ $Ti_3C_2T_x$ -NH_2 electrode material, obtained by Li et al. through the in situ growth of a two-dimensional bimetallic MOF-like structure, exhibits a high specific capacitance of 1924.00 $F \cdot g^{-1}$ (at 0.5 $A \cdot g^{-1}$) and demonstrates considerable cycling stability, withstanding 10000 cycles at a high current density of 10.0 $A \cdot g^{-1}$(Figure 14a, 14b, 14c, 14d). When utilised in an AC ASCs device, this assembled Ni/Co-MOF@TCT-NH_2 exhibited a maximum specific energy density of 98.1 $Wh \cdot g^{-1}$ at 600 $W \cdot g^{-1}$, with a coulombic efficiency maintained at approximately 99.3%. After 15,000 cycles, the coulombic efficiency remained at approximately 99.3%. All these outstanding electrochemical properties are attributed to the synergistic effect of double-layer capacitance and Faradaic pseudocapacitance [34].

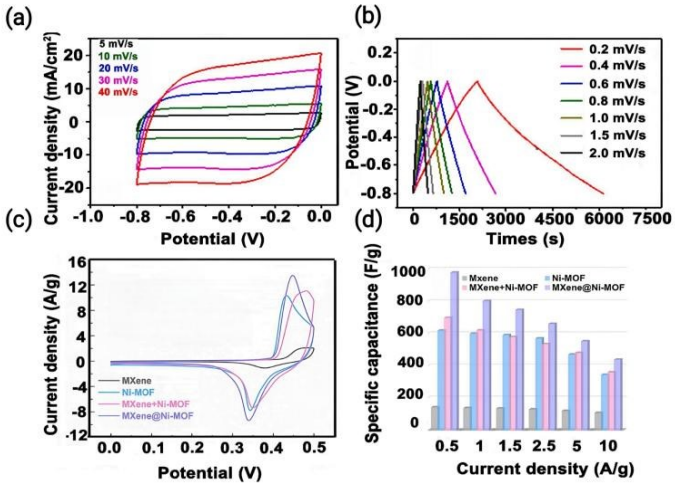

Figure 14. Electrochemical performance metrics of the Ni-MOF/ $Ti_3C_2T_x$ hybrid electrode derived from galvanostatic charge-discharge (GCD) measurements.

The table summarizes the corresponding specific capacitance values obtained at varying current densities. Notably, the composite delivers a high specific capacitance of approximately 1000 F/g at a current density of 1 A/g, which is consistent with the enhanced electrochemical activity reported for this heterostructure (typically 867.3 F/g). The systematic decrease in specific capacitance with increasing current density reflects the diffusion-limited kinetics inherent to Faradaic redox processes at higher rates. The robust capacitance retention observed across the measured current range underscores the beneficial role of the $Ti_3C_2T_x$ MXene conductive framework, which mitigates the internal resistance and facilitates rapid charge propagation within the Ni-MOF matrix. Data reproduced from Ref.

In summary, the synergistic mechanism between double-layer capacitance and pseudocapacitance in MOF@MXene composites fully exploits the structural and performance advantages of MXene and MOF (Figure 15a,15b). This synergy not only enhances the performance of supercapacitors but also offers broad prospects for their application in high-performance energy storage devices. With further research and technological advancements, MOF@MXene composites are expected to play an increasingly significant role in the field of supercapacitors.

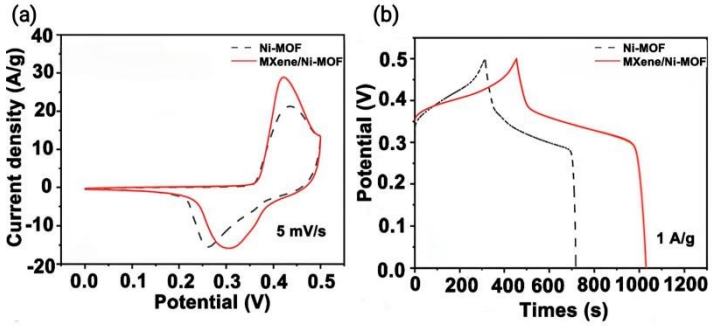

Figure 15. Comparative summary of current density responses as a function of applied potential for pristine Ni-MOF and the Ni-MOF/ $Ti_3C_2T_x$ (denoted as MXene/ Ni-MOF) composite electrode.

The data, extracted from cyclic voltammetry (CV) or linear sweep profiles, reveal a markedly enhanced current density for the composite material across the entire potential window. This pronounced increase in current response is directly attributed to the incorporation of the highly conductive $Ti_3C_2T_x$ MXene framework, which establishes efficient electron transport pathways and facilitates rapid Faradaic redox reactions at the electroactive Ni-MOF centers. Consequently, the MXene/ Ni-MOF hybrid exhibits significantly reduced charge transfer resistance and improved electrochemical utilization of the active material compared to the intrinsically insulating pristine Ni-MOF. Data adapted from Ref.

Applications of MOF@MXene composites in lithium-ion batteries

Pathways for the insertion and extraction of lithium ions in composite materials

The kinetics of lithium-ion insertion and extraction in MOF@MXene composites are primarily governed by the structural characteristics of their constituent materials. Metal-organic frameworks (MOFs), owing to their high specific surface area, pore size distribution, and abundance of unsaturated metal coordination sites, provide ample active sites for lithium-ion insertion. However, their inherently poor electrical conductivity severely hampers the kinetics of electrochemical reactions. In contrast, two-dimensional transition metal carbonitride (MXene) materials exhibit excellent electrical conductivity and unique interlayer channels for rapid ion transport; simultaneously, their surfaces are rich in functional groups (such as -OH and -F), endowing these materials with excellent solvent dispersibility. Therefore, by creating a MOF@MXene heterostructure, it is possible to combine the advantages of both materials whilst overcoming their respective drawbacks.

During the charging and energy storage process of lithium-ion batteries, lithium ions first interact with the negatively charged functional groups on the MXene

surface; as these functional groups provide abundant active sites, simultaneously, functional groups on the MXene surface (such as -OH or -F) may form coordinate bonds with metal ions within the MOF framework, creating new lithium-ion insertion sites. Consequently, compared to the amount of lithium ions that can be adsorbed by MXene alone, MOF@MXene can adsorb a significantly greater amount of lithium ions, thereby substantially enhancing the specific capacity of the lithium-ion battery, Significant progress has been made in this area in the laboratory. For example, the three-dimensional composite material Co@MXene/ CNF, prepared by Chen et al., consists of Co nanoparticles encapsulated within a 2D Ti3C2 MXene-wrapped MOF framework and embedded in N-doped carbon nanofibres (CNFs) [35]. This material demonstrates high initial discharge specific capacity (1.16323 Ah/g) and good capacity retention, as the Co nanoparticles provide additional reaction sites and enhance the reversible intercalation/ deintercalation, whilst the MXene and carbon nanofibres in this structure provide dual electron transport pathways. Consequently, the material exhibits a high initial discharge specific capacity of 1.16323 Ah/g and excellent capacity retention [36]. The Nb_4C_3TX MXene prepared by Qi Tang et al. using a water-assisted supercritical etching method exhibits an initial discharge specific capacity of approximately 0.43000 Ah/g which is one of the highest values reported for pure MXene anodes, and is approximately 0.73300 Ah/g lower than that of composite materials [37].

The lithium ions then penetrate into the interior of the MXene. Generally speaking, MOF@MXene composites typically exhibit an expanded interlayer spacing of over 10 Å, representing a significant increase of 3-4 Å compared to the 6-7 Å interlayer spacing of the original MXene material. It is evident, therefore, that MOF@MXene composites provide ample embedding space for lithium ions entering the interior of MXene via interlayer channels, thereby significantly enhancing the performance of lithium-ion batteries. For instance, a novel Co-MOF/V_2CT_x composite designed by Wu et al., in which Co-MOF is grown in situ on the surface and within the interlayers of V_2CT_x MXene, exhibits a larger interlayer spacing. Furthermore, the MOF within the composite provides additional specific capacity whilst effectively preventing the restacking of V_2CT_x MXene, thereby exposing more lithium-ion active sites and conferring greater specific capacity to the battery. Specifically, when this material is used as the battery anode, it exhibits a high specific capacity of 0.48400 Ah/g after 120 cycles at 0.1 A/g [38].

The lithium ions subsequently migrate through the MOF channels into the interior of the framework. Nitrogen adsorption-desorption analyses conducted by Maida Murtaza et al. revealed that the MOF@MXene composite possesses a specific surface area of 14.6 m^2/g, exceeding both the specific surface area of the pristine MXene (3.0 m^2/g) and that of pure MOF (11.2 m^2/g) [39]. In the MOF@ MXene composites, the hierarchical porosity of the MOF (classified into micropores (<2 nm), mesopores (2-50 nm) and macropores (>50 nm) based on size and geometry) remains structurally intact. Furthermore, the integration of MXene nanosheets optimises these pore structures, synergistically enhancing the material's ability to provide abundant adsorption sites for lithium ions. During ion diffusion, lithium ions form coordination interactions with metal ions or functional groups within the MOF framework, thereby enabling stable energy storage through local charge redistribution [39].

The discharge process of a lithium-ion battery is essentially the reverse of the charging process. Lithium ions are first desorbed from the internal pores of the MOF and re-enter the interlayer structure of the MXene via these pores. Subsequently, the lithium ions move relatively easily within the interlayer structure of the MXene, which has interlayer spacings ranging from a few nanometres to tens of nanometres; this facilitates the rapid release of lithium ions and reduces diffusion resistance. Finally, the lithium ions rapidly escape from the interlayer structure of the MXene.

In summary, the insertion process involves lithium ions adsorbing onto the surface of MXene, entering the interior of MXene via interlayer channels, and subsequently passing through the MOF channels into the interior of the MOF, where they interact with the metal ions and ligands of the MOF, enabling the energy to be stabilised. Conversely, the desorption process involves

lithium ions first desorbing from the internal pores of the MOF and re-entering the MXene through these same channels, allowing the ions to move freely between the MXene layers before escaping back into the electrolyte.

Table 3. Summary of synthesis methods and electrochemical performance of MOF/MXene composites.

Mof@Mxene composite			Reaction environment	Battery performance	References
Mofingredients	Mxeneingredients	Synthesis method	/	/	/
ZIF-67	Ti_3AlC_2 MXene	Electrospinning technology	First, $Ti_3C_2T_x$ MXene nanosheets were prepared from the Ti_3AlC_2 MAX phase; these were then subjected to self-assembly with Co-MOF via ultrasonication in an ice bath, and PAN was added to form a spinning solution; A nanofibre mat is obtained via electrospinning under specific conditions, followed by air stabilisation and argon carbonisation to convert the PAN into N-doped CNFs and the Co-MOF into Co nanoparticles, thereby forming Co@MXene/ CNFs; finally, the material is cut into self-supporting electrodes of a specific size and vacuum-dried.	Initial discharge capacity: 1163.23 mAh/g (1 A/g) Cycle performance: Reversible capacity retention of 422.80 mAh/g (500 cycles at 1 A/g)	[36]
$NiCl_2·6H_2O$	$SnCl_2·2H_2O$	Preparation of Ni cores by spray pyrolysis and preparation of Ni@SnNi core-shell structures by redox reactions	First, the Ni core was prepared via spray pyrolysis: a specific amount of $NiCl_2·6H_2O$ was dissolved in ethanol to form a precursor solution; after atomisation, the solution was introduced into a 1000 °C tube furnace and pyrolysed under an N_2H_2 atmosphere (residence time of approximately 1 s); the resulting Ni nanoparticles were collected using a microporous filter membrane; Next, the	Initial charge/discharge capacity: Ni@SnNi-6h: 0.900/0.693 $Ah·g^{-1}$ Ni@SnNi-9h: 0.900/0.703 $Ah·g^{-1}$ Cycle performance: Ni@SnNi-6h: Reversible capacity retention ≈ 0.570 $Ah·g^{-1}$ (300 cycles at 273.65K) Ni@SnNi-9h: Reversible capacity retention ≈ 0.570 $Ah·g^{-1}$ (300 cycles at 273.65K) Lithiumion diffusion	[40]

Mof@Mxene composite			Reaction environment	Battery performance	References
Mofingredients	Mxeneingredients	Synthesis method	/	/	/
			Ni@SnNi core-shell structure was prepared via a redox reaction: three equal portions of the Ni cores were dispersed in deionised water; a solution of $SnCl_2·2H_2O$ at specific concentrations was added to each, followed by ultrasonication; the mixtures were reacted for 6 h, 9 h and 12 h respectively; the corresponding samples were obtained after centrifugation and washing; Furthermore, by mixing Ni@SnNi-9h with commercial graphite in a specific mass ratio, a composite anode can be prepared.	coefficient (EIS calculation): Ni@SnNi-6h: 3.8×10-8 $cm^2·s^{-1}$ Ni@SnNi-9h: 8.7×10-8 $cm^2·s^{-1}$	
UiO-66	V_2AlC	Solvothermal and in situ selenation processes	Preparation of V_2CT_x: V_2AlC powder was mixed with hydrofluoric acid; after initial stirring, the mixture was stirred at a constant temperature to remove aluminium ions. The black residue was centrifuged, washed with water, and the pH adjusted, followed by vacuum freeze-drying to obtain the product. Preparation of the UiO-66/V_2CT_x precursor: The two raw materials and V_2CT_x were dissolved in DMF and sonicated; glacial acetic acid was added dropwise whilst continuing sonication, followed by a hydrothermal reaction; the precipitate was	Cycle performance (at high current density): Reversible capacity retention of 0.430 $Ah·g^{-1}$ (1,000 cycles at 1.0 $A·g^{-1}$) Charge transfer resistance (post-cycling): Rct of VSe_2-ZrO_2/C/MXene = 13.2 Ω (after 100 cycles)	[41]

Mof@Mxene composite			Reaction environment	Battery performance	References
Mofingredients	Mxeneingredients	Synthesis method	/	/	/
			washed with DMF and vacuum-dried to obtain the precursor. Preparation of VSe_2-ZrO_2/C/MXene composite: The precursor and selenium powder were mixed in the specified ratio and placed in a quartz boat; the product was obtained by high-temperature calcination under a nitrogen atmosphere. Under the same selenation conditions, heating UiO-66 and V_2CT_x separately yielded the corresponding products.		
$NiCl_2$	$Ti_3C_2T_x$	/	$Ti_3C_2T_x$ nanosheets: The powder was etched by reaction with a LiF-HCl mixture; the precipitate was washed with water, centrifuged and the pH adjusted, followed by ultrasonic dispersion and further centrifugation, and finally freeze-dried to yield the product. NF-MOF@MXene: $Ti_3C_2T_x$ nanosheets were mixed with a solution of metal ions and a ferrocene dicarboxylate-DMF solution, then heated in a high-pressure reactor. The precipitate was washed and vacuum-dried (with MXene constituting approximately 10.0%); the procedure for pure NF-MOF was identical, except that $Ti_3C_2T_x$ nanosheets were not added.	Capacitance: NF-MOF@MXene electrode: 0.620 $Ah \cdot g^{-1}$ (1 $A \cdot g^{-1}$), 0.478 $Ah \cdot g^{-1}$ (2 $A \cdot g^{-1}$), 0.375 $Ah \cdot g^{-1}$ (3 $A \cdot g^{-1}$), 0.195 $Ah \cdot g^{-1}$ (5 $A \cdot g^{-1}$)	[35]

Mof@Mxene composite			Reaction environment	Battery performance	References
Mofingredients	Mxeneingredients	Synthesis method	/	/	/
TCPP acts as an organic linker and forms a MOF structure by coordinating with metal V ions	V_2CT_x	/	V_2CT_x MXene: V_2AlC powder was etched with hydrofluoric acid; the precipitate was centrifuged, washed with water and the pH adjusted, followed by intercalation with tetramethylammonium hydroxide solution at room temperature. After repeated centrifugation, the precipitate was dispersed in deionised water and centrifuged again; the supernatant was collected to obtain the MXene dispersion. MOF@MXene heterostructure: The precipitate obtained by centrifuging the MXene dispersion was mixed with tetra (4-carboxyphenyl) porphyrin and N,N-dimethylformamide, transferred to an autoclave for reaction under heat, rapidly cooled, and the precipitate collected by centrifugation. Following washing with methanol, the material was vacuum-dried at room temperature.	The charge transfer resistances Rct are 5.26 Ω and 56.8 Ω respectively	[42]

The effect of MOF@MXene on cycling stability

In recent years, MOF@MXene heterostructures have demonstrated significant advantages in applications as anode materials for lithium-ion batteries (Figure 16a, 16b, 16c). Taking the research by Sun et al. as an example, the NF-MOF@MXene heterostructure they prepared demonstrated excellent rate performance as an anode material: At current densities of 1, 2, 3 and 5 $A \cdot g^{-1}$, the specific capacities reached 620, 478, 375 and 195 $mAh \cdot g^{-1}$ respectively, which is significantly superior to those of the single NF-MOF electrode (0.498, 0.327, 0.23 and 0.117 $Ah \cdot g^{-1}$).

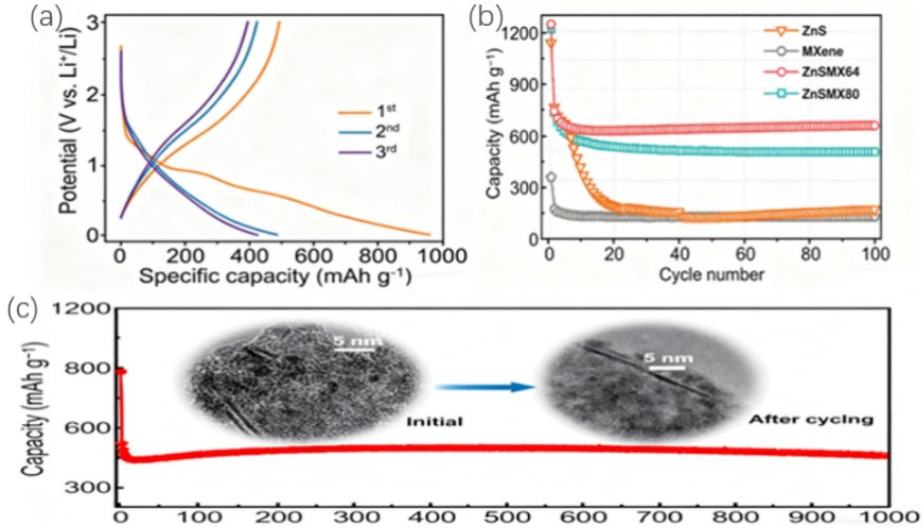

Figure 16. Electrochemical performance and structural characterization of the ZnSMX composite: (a) Cyclic voltammetry curves of the ZnSMX electrode at a scan rate of 0.1 mV s-1; (b) Cycling performance of ZnS, MXene, ZnSMX64, and ZnSMX80 electrodes at a current density of 0.5 A g^{-1}; (c) Long-term cycling stability of the ZnSMX electrode at 0.5 A g^{-1}. Insets: Transmission electron microscopy images of the electrode before and after cycling, demonstrating its structural integrity.

Furthermore, this material demonstrates particularly outstanding performance in terms of long-term cycling stability. Wu et al. further validated the advantages of this structure by constructing a heterojunction between a conductive ferrocene-based MOF (NF-MOF) and $Ti_3C_2T_x$ MXene. Specifically, after 5,000 cycles at a high current density of 5 A/g, the capacity retention rate remained as high as 80.0%, far exceeding that of either MXene or MOF materials alone (Figure 17a, 17b, 17c). The study indicates that this high performance is primarily attributed to the charge transfer at the interface between MXene and NF-MOF, which significantly enhances Li^+ storage capacity and structural stability, thereby improving cycling performance [43].

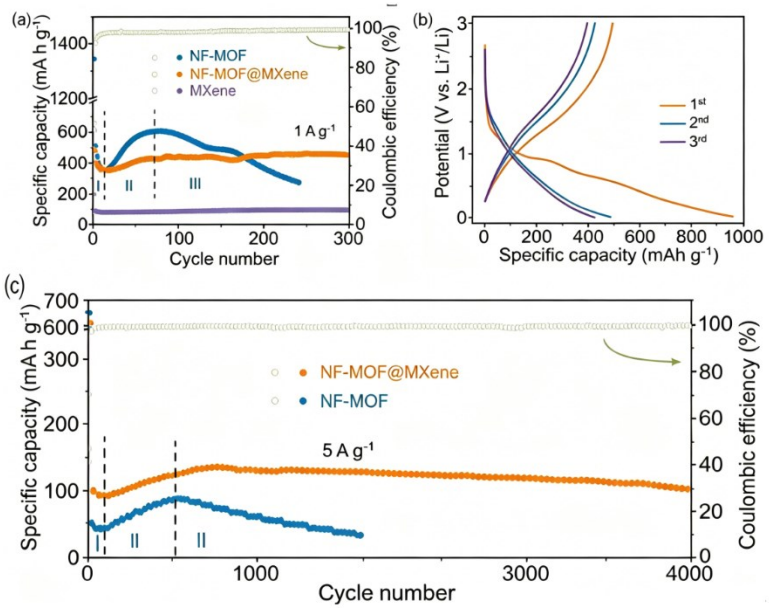

Figure 17. Electrochemical performance of the NF-MOF@MXene composite: (a) Cycling performance and Coulombic efficiency of NF-MOF, NF-MOF@MXene, and MXene electrodes at a current density of 1 A·g^{-1}; (b) Galvanostatic charge-discharge profiles of the NF-MOF@MXene electrode for the first three cycles at 0.1 A·g^{-1}; (c) Long-term cycling stability comparison between NF-MOF@MXene and NF-MOF electrodes at a high current density of 5 A·g^{-1}.

The mechanism by which interface engineering strategies improve cycling stability is elaborated in the work by Bin Cao et al. (Figure 17c). The researchers prepared a ZnS-MXene composite anode material by coordinating MXene with a MOF precursor (ZIF-8) to anchor ZnS nanodots onto the surface of $Ti_3C_2T_x$ MXene nanosheets. Electrochemical testing revealed that the material retained a specific capacity of 0.462 Ah g^{-1} after 1,000 cycles at a current density of 0.5 A g^{-1}. This performance is attributed to the interfacial interactions between MXene and ZnS: On the one hand, the anchoring effect on the MXene nanosheet surface suppressed the detachment of ZnS nanoparticles; on the other hand, the ZnS-MXene heterointerface exhibits high lithium adsorption capacity (ΔEads = -2.30 eV) and a low lithium diffusion energy barrier (0.18 eV), significantly facilitating the rapid migration and reversible storage of Li^+. Density functional theory (DFT) calculations further confirm that the electronic structure regulation at the heterointerface optimises the diffusion pathways for lithium ions, thereby achieving high cycling stability (Figure 18a-f) [44].

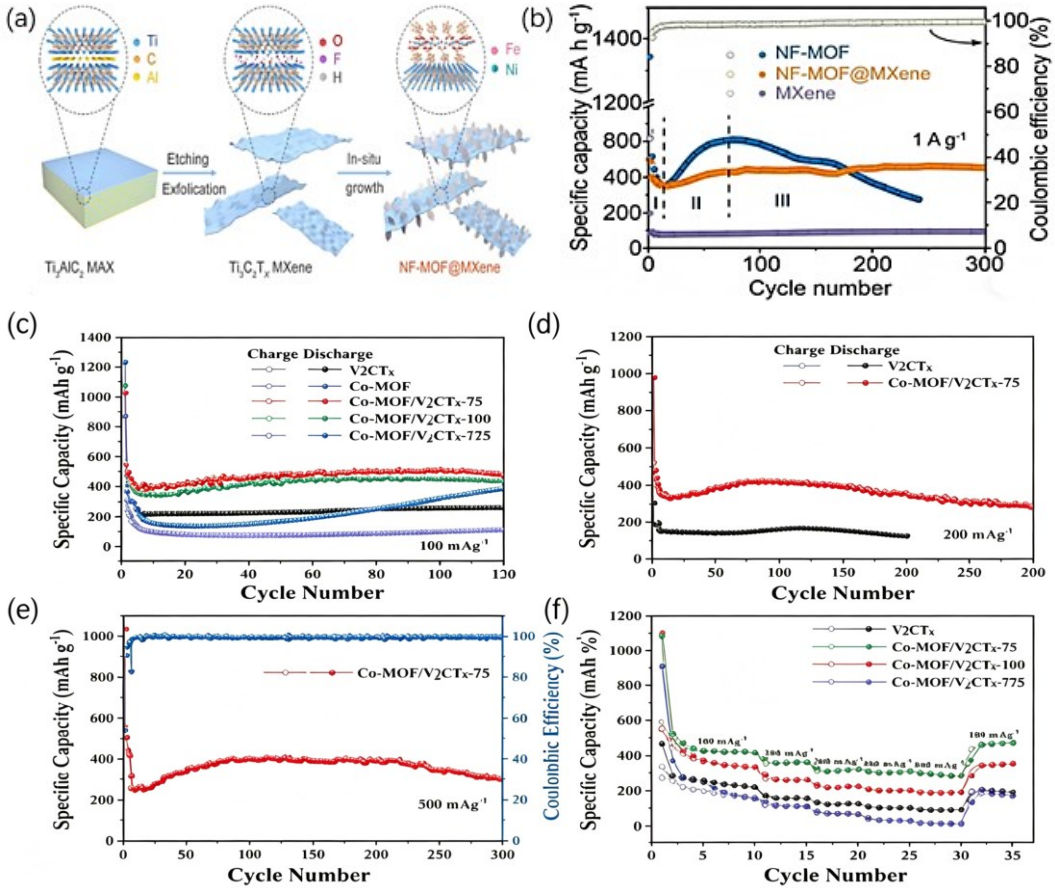

Figure 18. Synthesis and electrochemical performance of MXene-based composites: (a) Schematic illustration of the synthesis of NF-MOF@MXene via etching/exfoliation of Ti_3AlC_2 and in-situ growth of NF-MOF. (b) Cycling performance and Coulombic efficiency of NF-MOF, NF-MOF@MXene, and MXene electrodes at 1 A·g^{-1}. (c) Cycling performance of V_2CT_x, Co-MOF, and Co-MOF/ V_2CT_x composites with different ratios at 100 mA·g^{-1}. (d) Cycling comparison of V_2CT_x and Co-MOF/ V_2CT_x-75 electrodes at 200 mA·g^{-1};(e) Long-term cycling stability of Co-MOF/ V_2CT_x-75 electrode at 500 mA·g^{-1};(f) Rate capability of Co-MOF/ V_2CT_x composites with different ratios.

MOF@MXene diffusion coefficient

The diffusion coefficient is a key physical quantity describing the rate of diffusion of a substance in a medium. Its physical significance is defined as the amount of substance diffusing through a unit area per unit time under a unit concentration gradient; it is expressed in units of m^2/s or cm^2/s. This parameter essentially reflects

the mobility of molecules or atoms resulting from thermal motion and is a key factor determining the kinetic performance of lithium-ion batteries. Formula for calculating the lithium-ion diffusion coefficient based on electrochemical impedance spectroscopy (EIS):

$$D_{Li^+} = \frac{R^2T^2}{2\sigma^2A^2n^4F^4C^2} \quad (2)$$

D_{Li} represents the diffusion coefficient of lithium ions, S represents the surface area of the electrode/electrolyte, and n represents the number of electrons participating in the electrode reaction. R, T and F are the gas constant, absolute temperature and Faraday constant, respectively. C is the concentration of lithium ions.

In situ XRD and Raman spectroscopy analyses indicate that the VSe_2-ZrO_2/C/MXene composite electrode undergoes reversible structural evolution during charging and discharging. Upon lithium-ion insertion, the ZrO_2 lattice undergoes reversible expansion, forming the $LiXVSe_2$ phase; upon lithium-ion extraction, the lattice contracts and the $LiXVSe_2$ phase decomposes into the V/Li_2Se phase. A synergistic analysis confirms the reversible Li^+ intercalation mechanism, wherein the lattice distortion of ZrO_2 accommodates the strain induced by Li^+, whilst the conductive network of MXene synergistically facilitates ion transport [41].

In MOF@MXene composites, the presence of MXene significantly enhances the ion diffusion rate. The ZnS nanodot/MXene heterostructure prepared by Bin Cao et al. significantly increased the lithium ion diffusion coefficient; their experiments demonstrated that strong interactions form at the ZnS-MXene interface via Ti-O-Zn bonds, thereby lowering the lithium diffusion energy barrier. Through electrochemical kinetic analysis and DFT calculations, it was found that the lithium diffusion energy barrier at the ZnS-MXene heterojunction is lower than that in pure ZnS, and that the redistribution of charge density at the interface enhances electron mobility, thereby improving diffusion efficiency [45]. Yang's team and colleagues demonstrated via electrochemical impedance spectroscopy (EIS) that, compared with the pristine Sn-MOF, MXene@Sn-MOF exhibited a significantly reduced charge transfer resistance during the discharge activation process, decreasing from Rct = 95.4 Ω to Rct = 43.6 Ω; this is attributed to the excellent electronic conductivity of MXene, which facilitates interfacial charge transfer. Notably, the lithium ion diffusion coefficient D_{Li+} obtained via the Galvanostatic Intermittent Titration Technique (GITT) indicates that MXene@Sn-MOF exhibits significant improvement throughout the lithiation-delithiation process. During charge-discharge cycling, the evolution of the solid electrolyte interphase (SEI) stabilised, further confirming the enhanced stability of ion diffusion. These collective mechanisms endow MXene@Sn-MOF with the ability to accelerate lithium-ion diffusion and reduce polarisation resistance, which is directly related to its rate capability and cycling durability in lithium-ion battery applications [46].

Conclusion

The escalating demand for high-performance electrochemical energy storage (EES) systems has driven the exploration of advanced electrode materials that transcend the intrinsic limitations of conventional components. This review has provided a comprehensive analysis of the burgeoning field of MOF@MXene composites, delineating their synthesis strategies, synergistic charge storage mechanisms, and pivotal roles in supercapacitors and lithium-ion batteries (LIBs).

Summary and key findings

The strategic hybridization of metal-organic frameworks (MOFs) and two-dimensional transition metal carbides/nitrides (MXenes) represents a compelling paradigm to address the conductivity deficiency of pristine MOFs and the detrimental restacking and oxidation of MXenes. The principal conclusions drawn from this analysis are as follows:

Synergistic structural and electronic reinforcement: The integration of MOFs into MXene interlayers serves a dual purpose. The porous MOF architecture acts as a nanoscale spacer, effectively mitigating the van der Waals-induced restacking of MXene nanosheets and preserving electrolyte-accessible surface area. Reciprocally, the highly conductive MXene framework establishes continuous electron transport highways, compensating for the intrinsically poor electrical conductivity of MOFs. This interfacial synergy ensures robust structural integrity and accelerated charge transfer kinetics.

Optimized ion diffusion and storage kinetics: In supercapacitor applications, MOF@MXene heterostructures exhibit a cooperative interplay between electric double-layer capacitance (EDLC) and Faradaic pseudocapacitance. Surface-functionalized MXenes contribute rapid ion adsorption/desorption, while the redox-active metal centers in MOFs enable additional charge storage. The expanded interlayer galleries facilitate unimpeded ion diffusion, resulting in high specific capacitances and exceptional rate capabilities, as exemplified by Ni-MOF/ $Ti_3C_2T_x$ and Ni/Co-MOF@MXene systems.

Enhanced lithium-ion storage and cycling stability: For LIB anodes, MOF@MXene composites provide abundant Li^+ insertion sites and significantly lower diffusion energy barriers. The review elucidates the staged insertion/extraction pathways - from MXene surface adsorption to interlayer diffusion and subsequent MOF pore infiltration - which collectively enhance reversible capacity. Crucially, the robust heterointerface mitigates the volume expansion of MOFs and suppresses the detachment of active nanoparticles (e.g. ZnS nanodots), thereby conferring remarkable long-term cycling stability and high Coulombic efficiency.

Current challenges and bottlenecks

Despite the significant advancements, the translation of MOF@MXene composites from laboratory-scale investigations to practical EES devices faces several persistent challenges:

Scalable and green synthesis: The majority of reported synthesis protocols rely on batch hydrothermal/ solvothermal processes and the use of hazardous HF-based etchants for MXene preparation. The development of environmentally benign, cost-effective, and high-yield synthesis routes - such as molten salt etching or electrochemical exfoliation - remains a critical prerequisite for industrial viability.

Precise interfacial engineering: The exact nature of the chemical bonding at the MOF/ MXene heterointerface (e.g. Ti-O-C coordination) and its dynamic evolution during prolonged electrochemical cycling are not yet fully understood at the atomic scale. A deeper understanding is essential for the rational optimization of charge transfer efficiency and structural resilience.

Electrode architecture and mass loading: Most reported performance metrics are achieved with thin-film electrodes featuring relatively low mass loadings (<2 $mg \cdot cm^{-2}$). Achieving comparable gravimetric/volumetric performance at commercially relevant mass loadings (>10 $mg \cdot cm^{-2}$) while maintaining mechanical flexibility and wettability remains a substantial hurdle.

Chemical instability in aqueous and ambient environments: MXenes are inherently prone to oxidation in aqueous electrolytes and humid air, forming TiO_2 or other metal oxides that degrade conductivity and electrochemical activity. While MOF encapsulation offers partial protection, the long-term shelf-life and operational stability of MOF@MXene composites under realistic working conditions require further enhancement.

Future perspectives and research directions

To unlock the full potential of MOF@MXene composites for next-generation EES, future research should be directed toward the following avenues:

Machine learning-guided high-throughput screening: Given the vast compositional space of MOFs (metal nodes and organic linkers) and MXenes (transition metals and surface terminations), integrating density functional theory (DFT) calculations with machine learning algorithms could accelerate the prediction and discovery of optimal MOF/ MXene combinations with tailored electronic properties and adsorption energies for specific ions (Li^+, Na^+, K^+, Zn^{2+}).

Advanced in situ/operando characterization: Employing in situ X-ray diffraction (XRD), Raman spectroscopy, and transmission electron microscopy (TEM) is imperative to visualize the real-time structural evolution, ion intercalation dynamics, and SEI layer formation at the MOF@MXene interface during charge/discharge. Such insights will be invaluable for elucidating degradation mechanisms and guiding structural refinement.

Exploration of beyond-lithium systems: The unique open frameworks and tunable interlayer distances of MOF@MXene heterostructures position them as ideal candidates for emerging battery chemistries, including sodium-ion batteries (SIBs), potassium-ion batteries (PIBs), and aqueous zinc-ion batteries (AZIBs). The larger ionic radii in these systems may particularly benefit from the expanded interlayer spacing provided

by the MOF pillars.

Design of multifunctional thick electrodes: Future efforts should focus on constructing three-dimensional (3D) porous architectures, such as MXene/ MOF aerogels or 3D-printed scaffolds, that enable high mass loading without sacrificing ion/electron transport pathways. This approach bridges the gap between nanoscale material properties and macroscopic device performance.

Stability enhancement strategies: Beyond physical encapsulation, surface passivation strategies involving pre-intercalated cations (e.g. K^+, Mg^{2+}) or the application of ultra-thin protective coatings (e.g. carbon layers) should be integrated with MOF hybridization to synergistically enhance the oxidative stability of MXenes in aqueous and ambient environments.

In conclusion, MOF@MXene composites embody a promising frontier in materials chemistry for electrochemical energy storage. By addressing the current challenges related to scalable synthesis and interfacial stability, and by leveraging emerging computational and characterization tools, the rational design of these heterostructures is poised to deliver next-generation EES devices with unprecedented combinations of energy density, power capability, and cycling durability.

Funding

This work was supported by the Innovation Project at Ningxia University.

Acknowledgements

The authors would like to show sincere thanks to those techniques who have contributed to this research.

Conflicts of Interest

The authors declare no conflict of interest.

References

[1] Lv, Z., Li, W., Yang, L., Loh, X. J., Chen, X. (2019) Custom-made electrochemical energy storage devices. *ACS Energy Letters*, 4(2), 606-614.

[2] Yuan, S., Huang, X., Kong, T., Yan, L., Wang, Y. (2024) Organic electrode materials for energy storage and conversion: mechanism, characteristics, and applications. *Accounts of Chemical Research*, 57(10), 1550-1563.

[3] Du, R., Wu, Y., Yang, Y., Zhai, T., Zhou, T., Shang, Q., Zhu, L., Shang, C., Guo, Z. (2021) Porosity engineering of MOF-based materials for electrochemical energy storage. *Advanced Energy Materials*, 11(20), 2100154.

[4] Xie, L. S., Skorupskii, G., Dinca, M. (2020) Electrically conductive metal-organic frameworks. *Chemical Reviews*, 120(16), 8536-8580.

[5] Lin, X., Song, D., Shao, T., Xue, T., Hu, W., Jiang, W., Liu, N. (2024) A multifunctional biosensor via MXene assisted by conductive metal-organic framework for healthcare monitoring. *Advanced Functional Materials*, 34(11), 2311637.

[6] Ji, Y., Li, W., You, Y., Xu, G. (2024) In situ synthesis of M (Fe, Cu, Co and Ni)-MOF@ MXene composites for enhanced specific capacitance and cyclic stability in supercapacitor electrodes. *Chemical Engineering Journal*, 496, 154009.

[7] Yang, L., Cao, L. N., Li, S., Peng, P., Qian, H., Amaratunga, G., Wei, D. (2024) MOFs/MXene nano-hierarchical porous structures for efficient ion dynamics. *Nano Energy*, 129, 110076.

[8] Li, C., Shen, J., Wu, K., Yang, N. (2022) Metal centers and organic ligands determine electrochemistry of meta-organic frameworks. *Small*, 18(11), 2106607.

[9] Gao, M. L., Xue, T., Li, J., Guo, L., Zheng, H. Q., Lu, J., Jiang, H. L. (2025) The synthesis, characterization and applications of metal-organic frameworks. *Chinese Science Bulletin*, 71(2), 370-399.

[10] Duan, S., Qian, L., Zheng, Y., Zhu, Y., Liu, X., Dong, L., Zhang, J. (2024) Mechanisms of the accelerated Li+ conduction in MOF-based solid-state polymer electrolytes for all-solid-state lithium metal batteries. *Advanced Materials*, 36(32), 2314120.

[11] Hu, R., Li, Y. H., Zhang, Z. H., Fan, Z. Q., Sun, L. (2019) O-Vacancy-line defective Ti_2CO_2 nanoribbons: novel magnetism, tunable carrier mobility, and magnetic device behaviors. *Journal of Materials Chemistry C*, 7(25), 7745-7759.

[12] Theyagarajan, K., Kim, Y. J. (2024) Metal organic frameworks based wearable and point-of-care electrochemical sensors for healthcare monitoring.

Biosensors, 14(10), 492.

[13] Rahman, U. U., Humayun, M., Ghani, U., Usman, M., Ullah, H., Khan, A., Khan, A. (2022) MXenes as emerging materials: synthesis, properties, and applications. *Molecules*, 27(15), 4909.

[14] Das, P., Wu, Z. S. (2020) MXene for energy storage: present status and future perspectives. *Journal of Physics: Energy*, 2(3), 032004.

[15] Liu, S., Zhang, H., Chen, J., Peng, X., Chai, Y., Shao, X., Ding, B. (2025) Functionalization strategies of MXene architectures for electrochemical energy storage applications. *Energies*, 18(5), 1223.

[16] Devarayapalli, K. C., Lim, Y., Manchuri, A. R., Kim, B., Kim, G., Lee, D. S. (2024) Nickel 2-Methylimidazole Metal-Organic Framework Ultrathin Nanosheets/Titanium Carbide MXene Hybrid Nanostructure as a Bifunctional Electrocatalyst for Methanol and Urea Oxidation Reactions. *International Journal of Energy Research*, 2024(1), 8883022.

[17] Suganthi, S., Ahmad, K., Oh, T. H. (2024) Progress in MOFs and MOFs-integrated MXenes as electrode modifiers for energy storage and electrochemical sensing applications. *Molecules*, 29(22), 5373.

[18] Yu, K., Zhang, J., Hu, Y., Wang, L., Zhang, X., Zhao, B. (2024) Ni doped Co-MOF-74 synergized with 2D $Ti_3C_2T_x$ MXene as an efficient electrocatalyst for overall water-splitting. *Catalysts*, 14(3), 184.

[19] Khosroshahi, N., Bakhtian, M., Asadi, A., Safarifard, V. (2023) Revolutionizing energy storage: the emergence of MOF/MXene composites as promising supercapacitors. *Nano Express*, 4(4), 042002.

[20] Cai, Y., Chen, X., Xu, Y., Zhang, Y., Liu, H., Zhang, H., Tang, J. (2024) $Ti_3C_2T_x$ MXene/carbon composites for advanced supercapacitors: synthesis, progress, and perspectives. *Carbon Energy*, 6(2), e501.

[21] Wang, Y., Wang, Y., Jian, M., Jiang, Q., Li, X. (2024) MXene key composites: a new arena for gas sensors. *Nano-Micro Letters*, 16(1), 209.

[22] Ma, H., Luo, S., Cong, J., Yan, S. (2025) Applications of MOFs and their derivatives in lithium-oxygen battery cathodes: development and challenges. *Inorganics*, 13(2), 56.

[23] Tahir, B., Alraeesi, A., Tahir, M. (2024) Metal-organic framework (MOF) integrated Ti3C2 MXene composites for CO_2 reduction and hydrogen production applications: a review on recent advances and future perspectives. *Frontiers in Chemistry*, 12, 1448700.

[24] Zhang, X., Wang, Z., Guo, X. (2025) Confinement-induced Ni-based MOF formed on $Ti_3C_2T_x$ MXene support for enhanced capacitive Deionization of chromium (VI). *Scientific Reports*, 15(1), 3727.

[25] Prabhakar Vattikuti, S. V., Shim, J., Rosaiah, P., Mauger, A., Julien, C. M. (2023) Recent advances and strategies in MXene-based electrodes for supercapacitors: applications, challenges and future prospects. *Nanomaterials*, 14(1), 62.

[26] Zheng, B., Liu, X., Hua, Y. (2024) MOF-derived $ZnCo_2O_4$@ $Ti_3C_2T_x$ nanosheet with high microwave absorption. *Journal of Physics: Conference Series*, 2845(1), 012028.

[27] Zhuang, X., Zhang, S., Tang, Y., Yu, F., Li, Z., Pang, H. (2023) Recent progress of MOF/MXene-based composites: synthesis, functionality and application. *Coordination Chemistry Reviews*, 490, 215208.

[28] Thakur, K. K., Sharma, A. L., Singh, S. (2024) Exploring MXene-MOF composite for supercapacitor application. *Materials Chemistry and Physics*, 322, 129463.

[29] Du, Z., Liu, W., Liu, J., Chu, Z., Qu, F., Li, L., Shen, G. (2023) A thermally chargeable supercapacitor based on the g-C_3N_4-doped PAMPS/PAA hydrogel solid electrolyte and 2D MOF@ $Ti_3C_2T_x$ MXene heterostructure composite electrode. *Advanced Materials Interfaces*, 10(17), 2300266.

[30] Liu, C., Bai, Y., Li, W., Yang, F., Zhang, G., Pang, H. (2022) In situ growth of three-dimensional MXene/metal-organic framework composites for high-performance supercapacitors. *Angewandte Chemie International Edition*, 61(11), e202116282.

[31] Qu, Y., Shi, C., Cao, H., Wang, Y. (2020) Synthesis of Ni-MOF/$Ti_3C_2T_x$ hybrid nanosheets via ultrasonific method for supercapacitor electrodes.

Materials Letters, 280, 128526.

[32] Ramachandran, R., Rajavel, K., Xuan, W., Lin, D., Wang, F. (2018) Influence of $Ti_3C_2T_x$ (MXene) intercalation pseudocapacitance on electrochemical performance of Co-MOF binder-free electrode. *Ceramics International*, 44(12), 14425-14431.

[33] Wang, Y., Liu, Y., Wang, C., Liu, H., Zhang, J., Lin, J., Guo, Z. (2020) Significantly enhanced ultrathin NiCo-based MOF nanosheet electrodes hybrided with $Ti_3C_2T_x$ MXene for high performance asymmetric supercapacitor. *Engineered Science*, 9(12), 50-59.

[34] Hong, C. N., Crom, A. B., Feldblyum, J. I., Lukatskaya, M. R. (2023) Metal-organic frameworks for fast electrochemical energy storage: Mechanisms and opportunities. *Chem*, 9(4), 798-822.

[35] Sun, L., Wang, H., Zhai, S., Sun, J., Fang, X., Yang, H., Wu, H. (2023) Dual-conductive metal-organic framework@ MXene heterogeneity stabilizes lithium-ion storage. *Journal of Energy Chemistry*, 76, 368-376.

[36] Chen, Y., Cheng, J., Wang, A., Liu, C., Yan, H., Qiu, Y., Luo, Y. (2024) The enhanced performance of Li-ion batteries based on Co-MOF/MXene composites. *Inorganic Chemistry Communications*, 159, 111793.

[37] Tang, Q., Wang, Y., Chen, N., Pu, B., Qing, Y., Zhang, M., Yang, W. (2024) Ultra‐Efficient Synthesis of $Nb_4C_3T_x$ MXene via H_2O‐Assisted Supercritical Etching for Li‐Ion Battery. *Small Methods*, 8(3), 2300836.

[38] Gong, W., Li, S. Q., Gao, F., Lin, J., Ye, Y., Yang, X. R., Zhou, N. G. (2023) Tailoring composites via in situ growth of Co-MOF on V_2CT_x MXene as high-performance anode for lithium-ion batteries. *Solid State Ionics*, 399, 116295.

[39] Mathew, A. E., Jose, S., Babu, A. M., Varghese, A. (2024) State of the art MOF-composites and MXene-composites: synthesis, fabrication and diverse applications. *Materials Today Chemistry*, 36, 101927.

[40] Ji, H., Liu, Y., Du, G., Huang, T., Zhu, Y., Sun, Y., Pang, H. (2024) Synthesis and utilization of MXene/MOF hybrid composite materials. *Chemical Research in Chinese Universities*, 40(6), 943-963.

[41] Li, H., Li, J., Ma, L., Zhang, X., Li, J., Li, J., Pan, L. (2023) Heteroatomic interface engineering of an octahedron VSe_2-ZrO_2/C/MXene composite derived from a MXene-MOF hybrid as a superior-performance anode for lithium-ion batteries. *Journal of Materials Chemistry A*, 11(6), 2836-2847.

[42] Tan, Y., Yang, L., Zhai, D., Sun, L., Zhai, S., Zhou, W., Wu, H. (2022) MXene‐derived metal‐organic framework@ MXene heterostructures toward electrochemical NO sensing. *Small*, 18(50), 2204942.

[43] Yue, L., Chen, L., Wang, X., Lu, D., Zhou, W., Shen, D., Li, Y. (2023) Ni/Co-MOF@ aminated MXene hierarchical electrodes for high-stability supercapacitors. *Chemical Engineering Journal*, 451, 138687.

[44] Cao, B., Liu, H., Zhang, X., Zhang, P., Zhu, Q., Du, H., Xu, B. (2021) MOF-derived ZnS nanodots/$Ti_3C_2T_x$ MXene hybrids boosting superior lithium storage performance. *Nano-micro letters*, 13(1), 202.

[45] Yang, L., Cao, L. N., Li, S., Peng, P., Qian, H., Amaratunga, G., Wei, D. (2024) MOFs/MXene nano-hierarchical porous structures for efficient ion dynamics. *Nano Energy*, 129, 110076.

[46] Yang, Z., Weng, C., Gao, X., Meng, F., Ji, Y., Li, J., Pan, L. (2024) In situ construction of Sn-based metal-organic frameworks on MXene achieving fast electron transfer for rapid lithium storage. *Chemical Engineering Journal*, 486, 150299.